Electronic Supplementary Information (ESI) for:

Perylene Diimide-Based Cathode Interfacial Materials: Adjustable Molecular Structures and Conformation, Optimized Film Morphology, and Much Improved Performance of Non-Fullerene Polymer Solar Cells

Yaqin Li,[a] Mengmeng Han,[a] Wenli Yang,[a] Jing Guo,[b] Kai Chang,[a] Jiaqiang Wang,[a] Jie Min,*[b] Qianqian Li*[a] and Zhen Li*[ac]

[a] Sauvage Center for Molecular Sciences, Department of Chemistry, Wuhan University, Wuhan, 430072, China. E-mail: qianqian-alinda@163.com, lizhen@whu.edu.cn.
[b] The Institute for Advanced Studies, Wuhan University, Wuhan 430072, China. E-mail: min.jie@whu.edu.cn
[c] Institute of Molecular Aggregation Science, Tianjin University Tianjin 300072, China.

Table of Contents

1. General Information

Materials. Tetrahydrofuran and toluene were dried over and distilled from K-Na alloy under an atmosphere of dry argon. All chemicals were commercially available and used without further purification unless specially mentioned.

Instruments and Characterizations. ^{1}H and ^{13}C NMR spectra were characterized in deuterated solvents with a 400 MHz Bruker AVANCE III HD or 600 MHz WNMR-I NMR spectrometer at 298 K. The ten ionized compounds of **PDI-NBr** and **PDI-NO** series used the mixed solvent of CD_2Cl_2 and CD_3OD, and other compounds were characterized in $CDCl_3$. Chemical shifts were recorded with tetramethylsilane (TMS) as an internal standard. High resolution mass spectra (HRMS) were operated in a Thermo Fisher Scientific LTQ Orbitrap Elite or DIONEX UltiMate3000 & Bruker Compact mass spectrometer. Elemental analysis measurements were performed by a Perkin-Elmer microanalyzer analyzer. Thermal analysis was performed on NETZSCH STA449C thermal analyzer at a heating rate of 10 ^{o}C min^{-1} in nitrogen at a flow rate of 20 cm^3 min^{-1} for thermogravimetric analysis (TGA).

UV-vis spectra were obtained by a Shimadzu UV-2550 spectrometer. Fluorescence spectra were measured with a Hitachi F-4600 fluorescence spectrophotometer. Photoluminescence quantum yields and lifetimes were obtained by a FLS980 spectrometer. Cyclic voltammetry (CV) measurements were conducted on a CHI600A electrochemical workstation in a 0.1 mol/L acetonitrile solution of tetrabutylammonium hexafluorophosphate (Bu_4NPF_6) at a scan rate of 50 mV s^{-1}, by using a Pt wire, Ag/AgCl, and platinum column as the counter, reference, and working electrodes, respectively. In the above process, nitrogen gas was utilized for purging of the oxygen in the solvent. High-performance liquid chromatogram spectra were measured on an Agilent 1100 with 3% aqueous solution of trifluoroacetic acid and acetonitrile as the mobile phase. Electron paramagnetic resonance (EPR) spectra were recorded on a Bruker A200 EPR spectrometer. The X-ray diffraction (XRD) patterns were measured on a Rigaku Miniflex600 using Cu-Kα (λ = 1.5406 Å) radiation. SEM images were captured by a Zeiss SIGMA in 5 kV. The HOMO/LUMO distribution and optimal geometrics were calculated by the Gaussian 09 program at the B3LYP/6-31G* level.

Device Fabrication: The polymer solar cell devices were fabricated with a conventional configuration of ITO/PEDOT:PSS/J71:ITIC/Interlayer/Al. The ITO glasses, with the characteristic of ≤ 15 Ω/square, were purchased from Huananxiangcheng Technology Co. Ltd, Shenzhen. These ITO substrates were washed with toluene, DI water, acetone and isopropanol for 10 min each before use. After blown dry with high-purity nitrogen gas, the ITO glasses were treated by UV-Ozone for 15 min. Subsequently, the solution of PEDOT:PSS (purchased from Heraeus Holding GmbH), that had been filtered by a special filter (0.45 μm), was spin-coated (4000 rpm, 30 s) onto the cleaned ITO glass (~40 nm). Then, the devices were annealed at 150 ^{o}C for 15 min in air and taken to the glove box. The blend solution of J71:ITIC, as the active layer with the thickness of ~80 nm, was spin-coated onto the above obtained glass substrate (1500 rpm, 30 s), in which the weight ratio of J71 and ITIC was fixed at 1:1 and the concentration was 12 mg/mL in chloroform. After this, the active layers were annealed at 150 ^{o}C for 10 min. Then, pure methanol or methanol solution of PDI derivatives (1 mg/mL) was spin-coated onto the active layers (3000 rpm, 30 s). Finally, the Al electrode (100 nm) was deposited by thermal evaporation through a shadow mask under a vacuum of 5×10^{-6} mbar, and the active area was controlled to be 0.04 cm^2. An Enli Solar simulator (100 mW cm^{-2}) was utilized for characterizations of the current-voltage (*J*-*V*) curves under AM 1.5G irradiation. The illumination intensity of the light source was calibrated with a standard single-crystal Si solar cell (made by Enli Technology Co., Ltd, Taiwan, and calibrated by The National Institute of Metrology of China) to give a value of 100 mW cm^{-2} in the test. An Enli QE-R3011 (Enli Technology Co., Ltd Taiwan) was utilized for the measurement of EQE spectra, which was calibrated with a single-crystal silicon photovoltaic cell before use. The KLA-Tencor Model 300 profilometer was utilized for the measurements of film thicknesses.

The electrochemical impedance spectroscopy (EIS) measurements were also performed on a CS350 electrochemical workstation. The ultraviolet photoelectron spectra (UPS) were conducted with an ESCALAB250Xi photoelectron spectrometer with a -10 V bias. Atomic force microscopy (AFM) measurements were carried out with a Nano Wizard 4 atomic force microscopy (JPK Inc. Germany) in Qi mode to observe the surface morphologies of the fabricated devices. The contact angles were measured with a Contact Angle System OCA20 at ambient temperature with a 10 μL water droplet as the indicator. In addition, the hole and electron mobility of the devices were measured using the space charge limited current (SCLC) method. The structure of electron-only device is Glass/ITO/ZnO/J71:ITIC/Interlayer/Al, while that for the hole-only devices is Glass/ITO/PEDOT:PSS/J71:ITIC/Interlayer/MoOx/Ag. The mobility values were obtained by taking current-voltage curves and fitting the results to a space charge limited form.

2. Synthesis and Characterizations

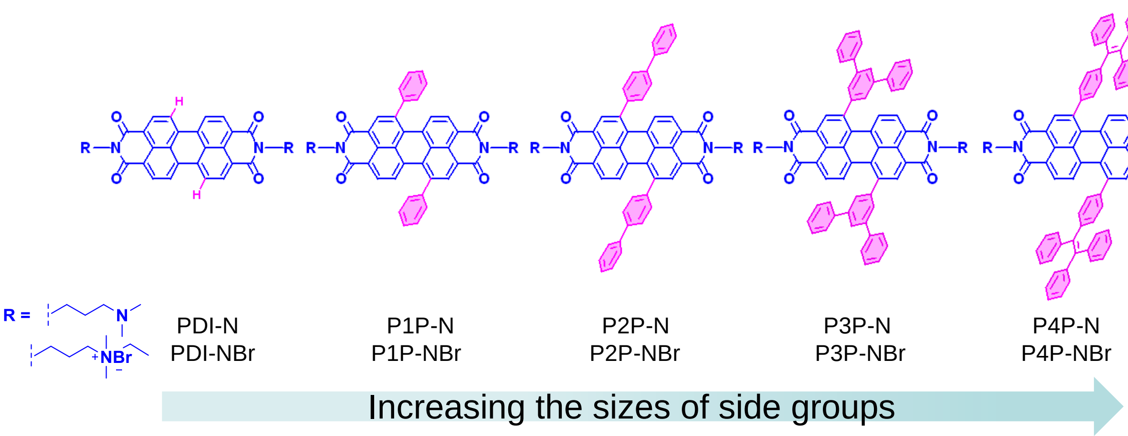

Chart S1. Molecular structures of the series of **PDI-N** and **PDI-NBr**.

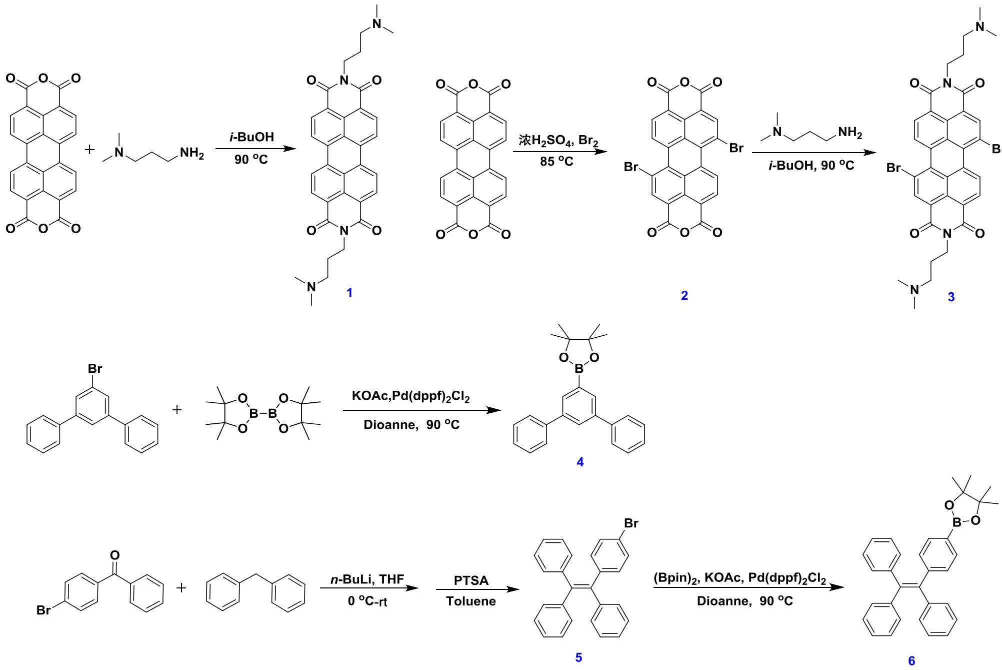

Scheme S1. Synthetic routes to the intermediates.

Compound 1: Synthesized according to the literature procedure.[1] ^{1}H NMR (600 MHz, $CDCl_3$, δ): 8.68-8.67 (d, J = 7.8 Hz, 4H, ArH), 8.61-8.59 (d, J = 8.4 Hz, 4H, ArH), 4.29-4.26 (t, J = 7.2 Hz, 4H, CH_2), 2.49-2.46 (t, J = 7.2 Hz, 4H, CH_2), 2.28 (s, 12H, CH_3), 1.99-1.94 (m, 4H, CH_2).

Compound 3: Compound **2** was synthesized according to our previous work.[2] Under an atmosphere of nitrogen, compound **2** (8.20 g, 15.00 mmol) was dissolved in *tert*-butanol (260 mL). *N*, *N*-Dimethyl-1, 3-propanediamine (4.16 mL, 33.00 mmol) was added and the reaction mixture was stirred at 90 °C for 24 h. After being cooled to room temperature, the reaction solution was poured into water, and then a red solid was precipitated. The red solid was separated by filtration, and washed repeatedly with water and ethanol. The crude product was purified by a silica gel column using CH_2Cl_2 : trimethylamine (50 : 1) as eluent to yield **3** as a red solid (6.55 g, 61%). ^1H NMR (400 MHz, $CDCl_3$, δ): 9.50-9.48 (d, J = 8.0 Hz, 2H, ArH), 8.93 (s, 2H, ArH), 8.72-8.70 (d, J = 8.0 Hz, 2H, ArH), 4.29-4.26 (t, J = 7.6 Hz, 4H, CH_2), 2.47-2.44 (t, J = 7.2 Hz, 4H, CH_2), 2.27 (s, 12H, CH_3), 1.98-1.90 (m, 4H, CH_2). ^{13}C NMR (100 MHz, $CDCl_3$, δ): 162.80, 162.30, 137.93, 132.85, 132.69, 129.94, 129.11, 128.43, 126.83, 123.07, 122.63, 120.80, 57.23, 45.46, 39.18, 26.06.

Compound 4: Under an atmosphere of nitrogen, 1-bromo-3,5-diphenylbenzene (3.09 g, 10.00 mmol), bis(pinacolato)diboron (3.81 g, 15.00 mmol), KOAc (3.44 g, 35.00 mmol), and Pd(dppf)$_2$Cl$_2$ (0.51 g, 0.70 mmol) were dissolved in 1,4-dioxane (100 mL). Then, the mixture was stirred at 90 °C for 42 h. After being cooled to room temperature, the solvent was evaporated under reduced pressure. The crude product was purified by a silica gel column using dichloromethane:petroleum ether (1 : 6) as eluent to yield **4** as a white solid (3.06 g, 86%). ^1H NMR (600 MHz, $CDCl_3$, δ): 8.03 (s, 2H, ArH), 7.90 (s, 1H, ArH), 7.69-7.68 (d, J = 7.8 Hz, 4H, ArH), 7.46-7.43(t, J = 7.8 Hz, 4H, ArH), 7.3-7.34 (t, J = 7.2 Hz, 2H, ArH), 1.38 (s, 12H, CH_3).

Compound 5 and **Compound 6:** Synthesized according to the literature procedure.[3] Compound **5**: ^1H NMR (400 MHz, $CDCl_3$, δ): 7.23-7.21 (d, J = 8.0 Hz, 2H, ArH), 7.15-7.08 (m, 9H, ArH), 7.04-6.99 (m, 6H, ArH), 6.92-6.86 (d, J = 8.0 Hz, 2H, ArH). Compound **6**: ^1H NMR (400 MHz, $CDCl_3$, δ): 7.55-7.53 (d, J = 8.0 Hz, 2H, ArH), 7.11-7.07 (m, 9H, ArH), 7.04-6.98 (m, 8H, ArH), 1.31 (s, 12H, CH_3).

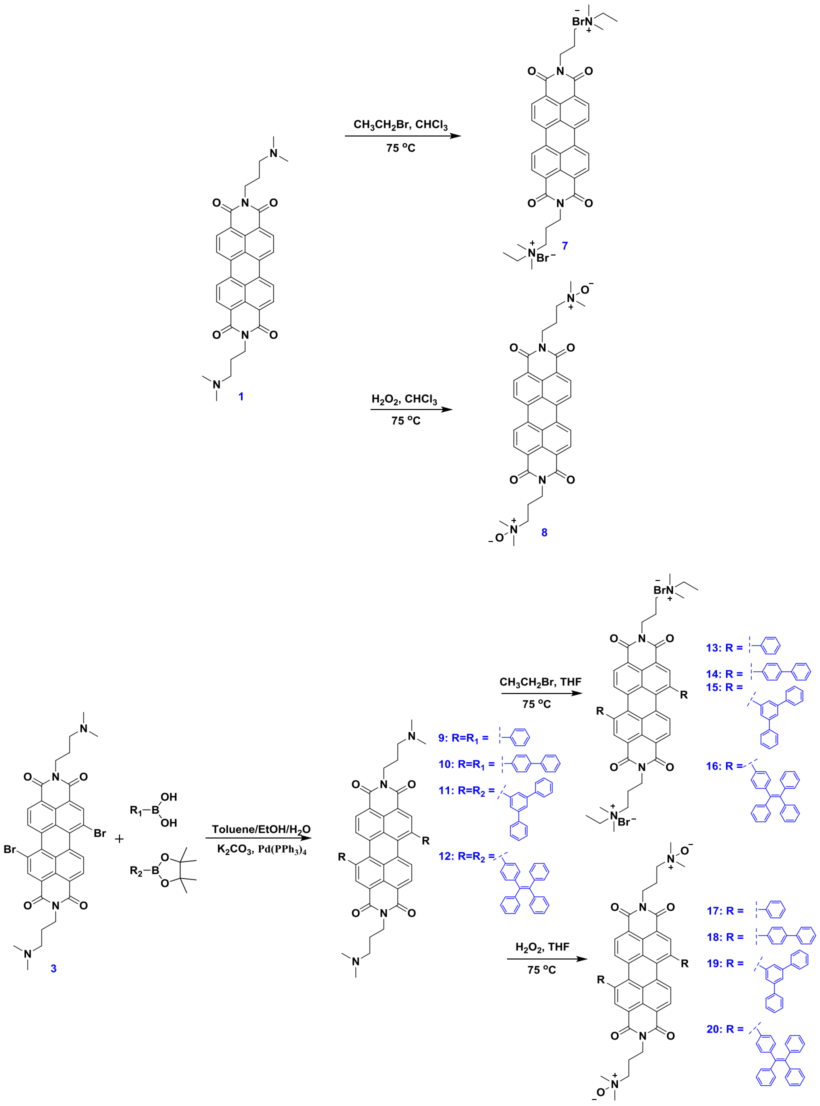

Scheme S2. Synthetic routes to water/alcohol-soluble PDI molecules.

Compound 7: Under an atmosphere of nitrogen, compound **1** (0.10 g, 0.18 mmol) was dissolved in chloroform (15 mL). After the addition of bromoethane (0.43 mL, 5.76 mmol), the mixture was stirred at 75 °C for 72 h. Then, after cooling to room temperature, solvents were removed under reduced pressure. The solid dissolved in methanol and precipitated into diethyl ether again. The collected red residue was further purified by dialysis and lyophilization to give **7** as a red solid (0.13 g, 96%). ^{1}H NMR (400 MHz, CD_3OD, CD_2Cl_2, δ): 7.68-7.67 (d, *J* = 4.8 Hz, 4H, ArH), 7.36 (br, 4H, ArH), 4.07 (br, 4H, CH_2), 3.69-3.62 (m, 8H, CH_2), 3.32 (s, 12H, CH_3), 2.31-2.29 (m, 4H, CH_2), 1.55-1.51 (t, *J* = 7.2 Hz, 6H, CH_3). ^{13}C NMR (150 MHz, CF_3COOD, δ): 167.57, 137.76, 134.99, 131.19, 128.03, 126.49, 124.03, 64.28, 63.32, 52.29, 40.32, 23.71, 9.12.

Compound 8: Under an atmosphere of nitrogen, compound **1** (0.10 g, 0.18 mmol) was dissolved in chloroform (15 mL). After the addition of 30% H_2O_2 (0.58 mL, 5.76 mmol), the mixture was stirred at 75 °C for 72 h. Then, after cooling to room temperature, solvents were removed under reduced pressure. The solid dissolved in methanol and precipitated into diethyl ether again. The collected red residue was further purified by dialysis and lyophilization to give **8** as a red solid (0.10 g, 93%). ^{1}H NMR (400 MHz, CD_3OD, CD_2Cl_2, δ): 8.16-8.14 (d, *J* = 8.0 Hz, 4H, ArH), 7.95-7.93 (d, *J* = 8.0 Hz, 4H, ArH), 4.27-4.24 (t, *J* = 6.8 Hz, 4H, CH_2), 3.54-3.50 (m, 4H, CH_2), 3.27 (s, 12H, CH_3), 2.43-2.36 (m, 4H, CH_2). HRMS (ESI) *m/z*: $[M + H]^+$ calculated for $C_{34}H_{32}N_4O_6$: 593.2395; Found: 593.2391.

Compound 9: Under an atmosphere of nitrogen, compound **3** (2.15 g, 3.00 mmol), phenylboronic acid (1.46 g, 12.00 mmol), K_2CO_3 (8.29 g, 60.00 mmol) and $Pd(PPh_3)_4$ (catalytic amount) were dissolved in toluene/ethanol/H_2O (60 mL/30 mL/15 mL). Then, the mixture was refluxed for 24 h. After being cooled to room temperature, the solution was concentrated via rotary evaporation. After dichloromethane extraction, the solvent was evaporated under reduced pressure. The crude product was purified by a silica gel column using CH_2Cl_2 : trimethylamine (100 : 1) as eluent to give **9** as purple solid (1.73 g, 81%). ^{1}H NMR (400 MHz, $CDCl_3$, δ): 8.64 (s, 2H, ArH), 8.16-8.14 (d, *J* = 8.0 Hz, 2H, ArH), 7.84-7.82 (d, *J* = 8.0 Hz, 2H, ArH), 7.57-7.54 (m, 4H, ArH), 7.52-7.49 (m, 6H, ArH), 4.26-4.22 (t, *J* = 8.0 Hz, 4H, CH_2), 2.46-2.43 (t, *J* = 7.2 Hz, 4H, CH_2), 2.27 (s, 12H, CH_3), 1.96-1.88 (m, 4H, CH_2). ^{13}C NMR (100 MHz, $CDCl_3$, δ): 163.33, 163.22, 141.87, 140.98, 135.12, 134.52, 132.24, 130.21, 129.19, 128.97, 128.74, 127.31, 122.04, 121.69, 57.23, 45.43, 38.98, 26.12. Anal. calcd for $C_{46}H_{40}N_4O_4$: C, 77.51; H, 5.66; N, 7.86. Found: C, 77.31; H, 5.79; N, 7.82. HRMS (ESI) *m/z*: $[M + H]^+$ calculated for $C_{46}H_{40}N_4O_4$: 713.3122; Found: 713.3129.

Compound 10: Prepared according to the similar procedure to compound **9** by using compound **3** (1.99 g, 2.80 mmol), 4 - biphenylboronic acid (1.65 g, 8.32 mmol), K_2CO_3 (7.74 g, 56.00 mmol) and $Pd(PPh_3)_4$ (catalytic amount). Purple solid (1.89 g, 78%). ^{1}H NMR (400 MHz, $CDCl_3$, δ): 8.67 (s, 2H, ArH), 8.19-8.17 (d, *J* = 8.0 Hz, 2H, ArH), 7.96-7.94 (d, *J* = 8.0 Hz, 2H, ArH), 7.76-7.70 (m, 8H, ArH), 7.65-7.63 (d, *J* = 8.4 Hz, 4H, ArH), 7.54-7.50 (t, *J* = 7.6 Hz, 4H, ArH), 7.44-7.71 (t, *J* = 7.6 Hz, 2H, ArH), 4.27-4.23 (t, *J* = 7.6 Hz, 4H, CH_2), 2.45-2.42 (t, *J* = 7.2 Hz, 4H, CH_2), 2.26 (s, 12H, CH_3), 1.96-1.88 (m, 4H, CH_2). ^{13}C NMR (100 MHz, $CDCl_3$, δ): 163.33, 163.22, 141.52, 140.73, 140.58, 139.89, 135.12, 134.56, 132.26, 130.23, 129.52, 129.25, 129.06, 129.01, 128.80, 127.93, 127.37, 127.11, 122.13, 121.79, 57.28, 45.49, 39.03, 26.18. Anal. calcd for $C_{58}H_{48}N_4O_4$: C, 80.53; H, 5.59; N, 6.48. Found: C, 80.64; H, 5.52; N, 6.65. HRMS (ESI) *m/z*: $[M + H]^+$ calculated for $C_{58}H_{48}N_4O_4$: 865.3748; Found: 865.3752.

Compound 11: Prepared according to the similar procedure to compound **9** by using compound **3** (1.43 g, 2.00 mmol), compound **4** (2.14 g, 6.00 mmol), K_2CO_3 (5.53 g, 40.00 mmol) and $Pd(PPh_3)_4$ (catalytic amount). Red solid (1.53 g, 75%). ^{1}H NMR (400 MHz, $CDCl_3$, δ): 8.76 (s, 2H, ArH), 8.22-8.20 (d, *J* = 8.0 Hz, 2H, ArH), 8.10-8.08 (d, *J* = 8.0 Hz, 2H, ArH), 7.95-7.94 (t, *J* = 1.6 Hz, 2H, ArH), 7.78-7.77 (d, *J* = 1.6 Hz, 4H, ArH), 7.67-7.65 (d, *J* = 7.6 Hz, 8H, ArH), 7.48-7.45 (m, 8H, ArH), 7.41-7.37 (m, 4H, ArH), 4.25-4.22 (t, *J* = 7.2 Hz, 4H, CH_2), 2.46-2.42 (t, *J* = 7.2 Hz, 4H, CH_2), 2.25 (s, 12H, CH_3), 1.95-1.88 (m, 4H, CH_2). ^{13}C NMR (100 MHz, $CDCl_3$, δ): 163.36, 163.30, 143.86, 143.23, 140.89, 140.18, 135.34, 134.70, 132.54, 130.46, 129.46, 129.17, 128.98, 128.01, 127.70, 126.48, 126.37, 122.32, 122.07, 57.24, 45.40, 39.01, 26.07. Anal. calcd for $C_{70}H_{56}N_4O_4$: C, 82.65; H, 5.55; N, 5.51. Found: C, 82.60; H, 5.42; N, 5.66. HRMS (ESI-QTOF) *m/z*: $[M + H]^+$ calculated for $C_{70}H_{56}N_4O_4$: 1017.4375; Found: 1017.4359.

Compound 12: Prepared according to the similar procedure to compound **9** by using compound **3** (1.56 g, 2.18 mmol), compound **6** (2.50 g, 5.46 mmol), K_2CO_3 (6.03 g, 43.60 mmol) and $Pd(PPh_3)_4$ (catalytic amount). Purple solid (2.26 g, 85%). ^{1}H NMR (400 MHz, $CDCl_3$, δ): 8.57 (s, 2H, ArH), 8.20-8.18 (d, *J* = 8.0 Hz, 2H, ArH), 7.84-7.82 (d, *J* = 8.0 Hz, 2H, ArH), 7.21-7.05 (m, 38H, ArH), 4.29-4.25 (t, *J* = 7.6 Hz, 4H, CH_2), 2.51-2.47 (t, *J* = 7.6 Hz, 4H, CH_2), 2.30 (s, 12H, CH_3), 1.99-1.92 (m, 4H, CH_2). ^{13}C NMR (100 MHz, $CDCl_3$, δ): 163.37, 163.21, 144.85, 143.67, 143.33, 143.21, 142.09, 140.79, 140.02, 139.88, 135.05, 134.53, 133.18, 132.19, 131.39, 131.28, 130.03, 128.96, 128.34, 128.07, 127.94, 127.78, 127.28, 127.10, 126.83, 126.74,121.97, 121.57, 57.24, 45.41, 38.92, 26.13. Anal. calcd for $C_{86}H_{68}N_4O_4$: C, 84.56; H, 5.61; N, 4.59. Found: C, 84.49; H, 5.59; N, 4.53. HRMS (ESI-QTOF) *m/z*: $[M + H]^+$ calculated for $C_{86}H_{68}N_4O_4$: 1221.5314; Found: 1221.5310.

Compound 13: Under an atmosphere of nitrogen, compound **9** (0.12 g, 0.17 mmol) was dissolved in tetrahydrofuran (15 mL). After the addition of bromoethane (0.41 mL, 5.44 mmol), the mixture was stirred at 75 °C for 72 h. Then, after cooling to room temperature, solvents were removed under reduced pressure. The solid dissolved in methanol and precipitated into diethyl ether again. The collected purple residue was then further purified by dialysis and lyophilization to give **13** (0.15 g, 95%). ^{1}H NMR (400 MHz, CD_3OD, CD_2Cl_2, δ): 8.52 (s, 2H, ArH), 8.16-8.14 (d, *J* = 8.0 Hz, 2H, ArH), 7.80-7.78 (d, *J* = 8.0 Hz, 2H, ArH), 4.33-4.30 (t, *J* = 6.8 Hz, 4H, CH_2), 3.54-3.50 (m, 4H, CH_2), 3.47-3.41 (m, 4H, CH_2), 3.11 (s, 12H, CH_3), 2.30-2.23 (m, 4H, CH_2), 1.43-1.39 (t, *J* = 7.2 Hz, 6H, CH_3). ^{13}C NMR (100 MHz, CD_3OD, CD_2Cl_2, δ): 163.42, 163.04, 141.38, 140.89, 134.52, 133.90, 131.74, 130.40, 130.26, 128.91, 128.77, 128.67, 128.36, 126.57, 121.30, 121.00, 61.61, 60.24, 50.14, 37.73, 21.69, 7.89. HRMS (ESI-QTOF) *m/z*: [M + H]$^+$ calculated for $C_{50}H_{50}Br_2N_4O_4$: 929.2272; Found: 929.2258.

Compound 14: Prepared according to the similar procedure to compound **13** by using compound **10** (0.12 g, 0.14 mmol) and bromoethane (0.33 mL, 4.48 mmol). Purple solid (0.14 g, 93%). ^{1}H NMR (400 MHz, CD_3OD, CD_2Cl_2, δ): 8.51 (s, 2H, ArH), 8.22-8.20 (d, *J* = 8.0 Hz, 2H, ArH), 7.89-7.87 (d, *J* = 8.0 Hz, 2H, ArH), 7.82-7.80 (d, *J* = 8.4 Hz, 4H, ArH), 7.75-7.73 (d, *J* = 7.2 Hz, 4H, ArH), 7.65-7.63 (d, *J* = 8.0 Hz, 4H, ArH), 7.54-7.51 (t, *J* = 7.6 Hz, 4H, ArH), 7.45-7.42 (t, *J* = 7.6 Hz, 2H, ArH), 4.36-4.32 (t, *J* = 6.8 Hz, 4H, CH_2), 3.57-3.53 (m, 4H, CH_2), 3.48-1.42 (m, 4H, CH_2), 3.12 (s, 12H, CH_3), 2.33-2.25 (m, 4H, CH_2), 1.43-1.39 (t, *J* = 7.2 Hz, 6H, CH_3). ^{13}C NMR (100 MHz, CD_3OD, CD_2Cl_2, δ): 163.45, 163.01, 141.63, 140.45, 140.23, 139.58, 134.36, 133.85, 131.67, 130.41, 129.24, 128.89, 128.67, 128.40, 127.91, 126.75, 126.56, 121.36, 121.08, 61.58, 60.16, 49.98, 37.77, 21.67, 7.76. HRMS (ESI-QTOF) *m/z*: [M + H]$^+$ calculated for $C_{62}H_{58}Br_2N_4O_4$: 1081.2898; Found: 1081.2634.

Compound 15: Prepared according to the similar procedure to compound **13** by using compound **11** (0.12 g, 0.12 mmol) and bromoethane (0.29 mL, 3.84 mmol). Purple solid (0.14 g, 96%). ^{1}H NMR (400 MHz, CD_3OD, CD_2Cl_2, δ): 8.33-8.31 (d, *J* = 8.4 Hz, 4H, ArH), 8.00-7.99 (d, *J* = 7.2 Hz, 2H, ArH), 7.90-7.41 (m, 26H, ArH), 4.35 (br, 4H, CH_2), 3.66-3.62 (m, 4H, CH_2), 3.43-3.38 (m, 4H, CH_2), 3.11 (s, 12H, CH_3), 2.39-2.32 (m, 4H, CH_2), 1.36-1.32 (t, *J* = 7.2 Hz, 6H, CH_3). ^{13}C NMR (100 MHz, CD_3OD, CD_2Cl_2, δ): 163.53, 162.84, 143.80, 142.48, 140.70, 139.69, 134.27, 133.50, 131.44, 131.03, 128.84, 128.52, 128.37, 127.96, 127.00, 126.43, 126.13, 121.52, 121.36, 61.69, 60.11, 50.01, 38.01, 21.71, 7.74. HRMS (ESI-QTOF) *m/z*: [M + H]$^+$ calculated for $C_{74}H_{66} Br_2N_4O_4$: 1233.3524; Found: 1233.3356.

Compound 16: Prepared according to the similar procedure to compound **13** by using compound **12** (0.12 g, 0.10 mmol) and bromoethane (0.24 mL, 3.20 mmol). Purple solid (0.14 g, 98%). ^{1}H NMR (400 MHz, CD_3OD, CD_2Cl_2, δ): 8.37 (s, 2H, ArH), 7.77-7.75 (d, *J* = 8.0 Hz, 2H, ArH), 7.49-7.47 (d, *J* = 7.2 Hz, 2H, ArH), 7.41-7.38 (t, *J* = 7.6 Hz, 4H, ArH), 7.29-7.27 (d, *J* = 8.4 Hz, 4H, ArH), 7.22-7.10 (m, 26H, ArH), 6.97-6.95 (d, *J* = 7.2 Hz, 4H, ArH), 4.40-4.36 (t, *J* = 6.8 Hz, 4H, CH_2), 3.66-3.64 (m, 4H, CH_2), 3.51-3.45 (m, 4H, CH_2), 3.16 (s, 12H, CH_3), 2.32-2.25 (m, 4H, CH_2), 1.44-1.41 (t, *J* = 7.2 Hz, 6H, CH_3). ^{13}C NMR (100 MHz, CD_3OD, CD_2Cl_2, δ): 163.21, 163.01, 144.97, 143.98, 143.13, 143.02, 142.21, 140.85, 140.11, 139.60, 134.87, 134.84, 133.04, 131.65, 131.38, 131.07, 131.01, 129.53, 128.06, 127.92, 127.81, 127.70, 127.36, 126.74, 126.62, 121.55, 120.70, 61.66, 60.22, 50.08, 37.68, 21.70, 7.87.

Compound 17: Under an atmosphere of nitrogen, compound **9** (0.12 g, 0.17 mmol) was dissolved in tetrahydrofuran (15 mL). After the addition of 30% H_2O_2 (0.55 mL, 5.44 mmol), the mixture was stirred at 75 °C for 72 h. Then, after cooling to room temperature, solvents were removed under reduced pressure. The solid dissolved in methanol and precipitated into diethyl ether again. The collected red residue was then further purified by dialysis and lyophilization to give **17** as a purple solid (0.12 g, 93%). ^{1}H NMR (400 MHz, CD_3OD, CD_2Cl_2, δ): 8.22 (s, 2H, ArH), 8.00-7.98 (d, *J* = 8.0 Hz, 2H, ArH), 7.49-7.35 (m, 12H, ArH), 4.35-4.32 (t, *J* = 6.8 Hz, 4H, CH_2), 3.54-3.50 (m, 4H, CH_2), 3.25 (s, 12H, CH_3), 2.42-2.35 (m, 4H, CH_2). ^{13}C NMR (100 MHz, CD_3OD, CD_2Cl_2, δ): 163.32, 163.06, 141.48, 140.79, 134.50, 133.83, 131.70, 130.20, 130.13, 128.69, 128.36, 126.62, 121.41, 121.15, 68.23, 57.54, 37.80, 22.47. HRMS (ESI) *m/z*: [M + H]$^+$ calculated for $C_{46}H_{40}N_4O_6$: 745.3021; Found: 745.3038.

Compound 18: Prepared according to the similar procedure to compound **17** by using compound **10** (0.12 g, 0.14 mmol) and 30% H_2O_2 (0.45 mL, 4.48 mmol). Purple solid (0.12 g, 95%). ^{1}H NMR (400 MHz, CD_3OD, CD_2Cl_2, δ): 8.38 (s, 2H, ArH), 8.11 (br, 2H, ArH), 7.77-7.73 (m, *J* = 8.0 Hz, 8H, ArH), 7.53-7.44 (m, 12H, ArH), 4.33 (br, 4H, CH_2), 3.53 (br, 4H, CH_2), 3.24 (s, 12H, CH_3), 2.40 (br, 4H, CH_2). ^{13}C NMR (100 MHz, CD_3OD, CD_2Cl_2, δ): 163.26, 162.97, 141.47, 140.28, 139.60, 134.37, 133.74, 131.60, 130.16, 129.18, 128.82, 128.73, 128.55, 128.34, 127.81, 126.73, 126.60, 121.40, 121.15, 68.11, 57.43, 37.84, 22.44. HRMS (ESI) *m/z*: [M + H]$^+$ calculated for $C_{58}H_{48}N_4O_6$: 897.3647; Found: 897.3657.

Compound 19: Prepared according to the similar procedure to compound **17** by using compound **11** (0.12 g, 0.12 mmol) and 30% H_2O_2 (0.39 mL, 3.84 mmol). Purple solid (0.11 g, 90%). ^{1}H NMR (400 MHz, CD_3OD, CD_2Cl_2, δ): 8.37 (s, 2H, ArH), 8.20 (br, 2H, ArH), 7.97 (br, 2H, ArH), 7.82-7.39 (m, 26H, ArH), 4.36 (br, 4H, CH_2), 3.60 (br, 4H, CH_2), 3.27 (s, 12H, CH_3), 2.44 (br, 4H, CH_2). ^{13}C NMR (150 MHz, CF_3COOD, δ): 169.38, 169.15, 147.90, 146.08, 145.60, 143.26, 140.05, 137.82, 134.92, 134.30, 132.70, 132.41, 132.25, 131.46, 131.18, 130.31, 130.04, 129.72, 124.37, 124.18, 71.10, 59.57, 41.39, 25.40. HRMS (ESI) *m/z*: [M + H]$^+$ calculated for $C_{70}H_{56}N_4O_6$: 1049.4272; Found: 1049.4178.

Compound 20: Prepared according to the similar procedure to compound **17** by using compound **12** (0.12 g, 0.10 mmol) and 30% H_2O_2 (0.32 mL, 3.20 mmol). Purple solid (0.12 g, 94%). ^{1}H NMR (400 MHz, CD_3OD CD_2Cl_2, δ): 8.33 (s, 2H, ArH), 7.66-7.64 (d, J = 7.6 Hz, 2H, ArH), 7.50-7.48 (d, J = 7.2 Hz, 2H, ArH), 7.41-7.38 (t, J = 7.6 Hz, 4H, ArH), 7.28-7.26 (d, J = 7.2 Hz, 4H, ArH), 7.21-7.10 (m, 26H, ArH), 6.89-6.88 (d, J = 6.8 Hz, 4H, ArH), 4.38-4.34 (t, J = 6.8 Hz, 4H, CH_2), 3.55-3.51 (m, 4H, CH_2), 3.24 (s, 12H, CH_3), 2.43-2.36 (m, 4H, CH_2). ^{13}C NMR (100 MHz, CD_3OD, CD_2Cl_2, δ): 163.17, 162.97, 144.86, 143.94, 143.18, 143.05, 142.17, 140.73, 140.14, 139.68, 134.77, 133.61, 132.99, 131.49, 131.32, 131.05, 130.99, 129.51, 128.08, 127.77, 127.64, 127.38, 126.66, 121.63, 120.84, 67.90, 57.41, 37.82, 22.36. HRMS (ESI-QTOF) *m/z*: $[M + H]^+$ calculated for $C_{86}H_{68}N_4O_6$: 1253.5212; Found: 1253.5154.

3. Figures and Tables

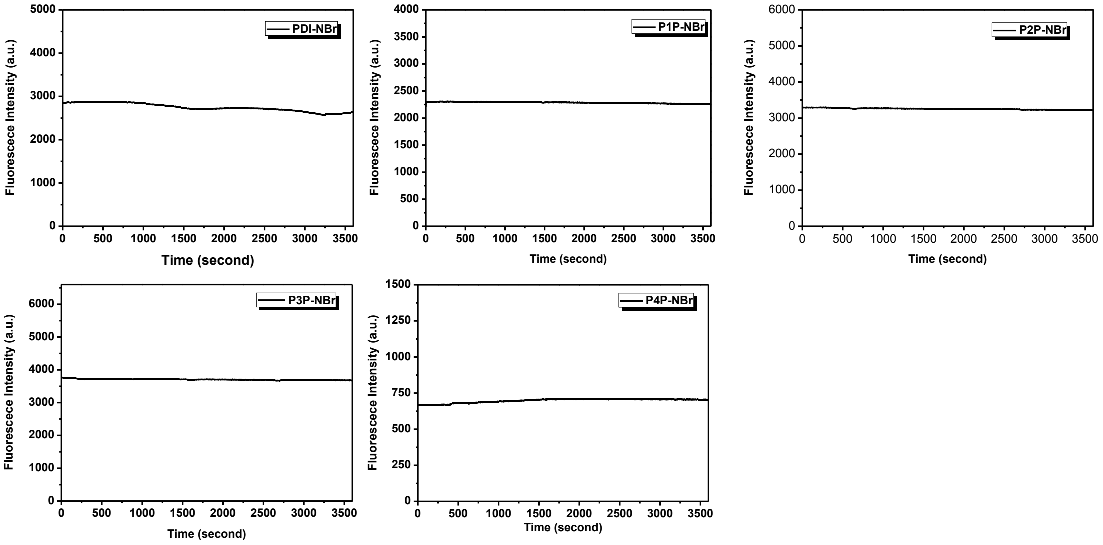

Figure S1. The fluorescence intensity of **PDI-NBr** series in methanol solution (concentration: 2 × 10^{-5} mol/L) with increasing scan (0-3600 s) under optimal excitation wavelength irradiation.

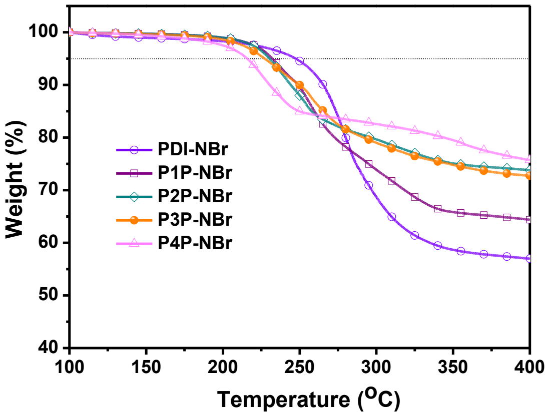

Figure S2. Thermogravimetric analyses (TGA) curves of **PDI-NBr** series.

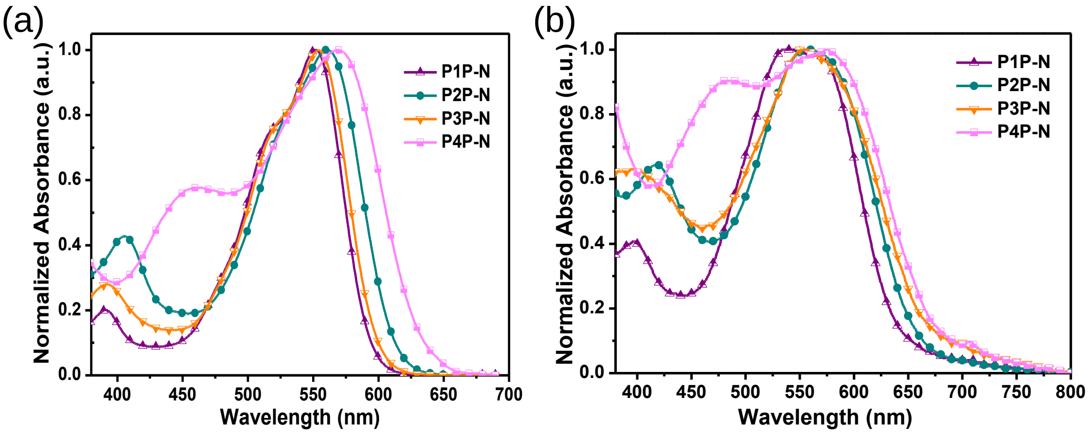

Figure S3. UV-vis absorption spectra of the **PDI-N** series in DCM solution (concentration: 2×10^{-5} mol/L) (a) and film states (b).

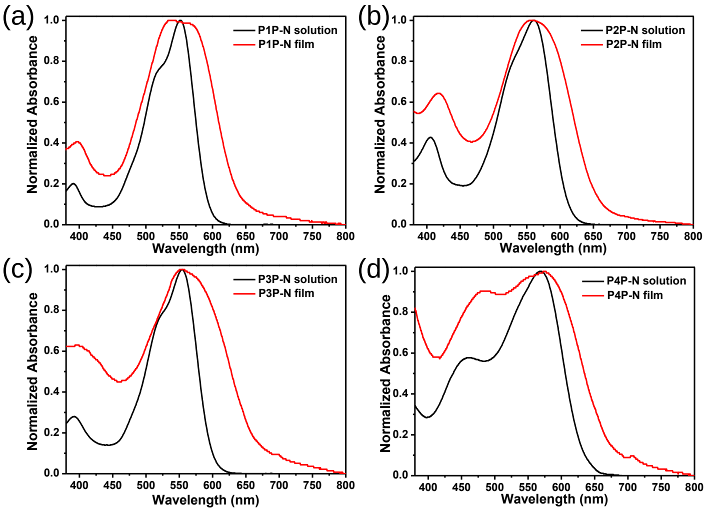

Figure S4. UV-vis absorption spectra of the **PDI-N** series in DCM solution (concentration: 2×10^{-5} mol/L) and film states.

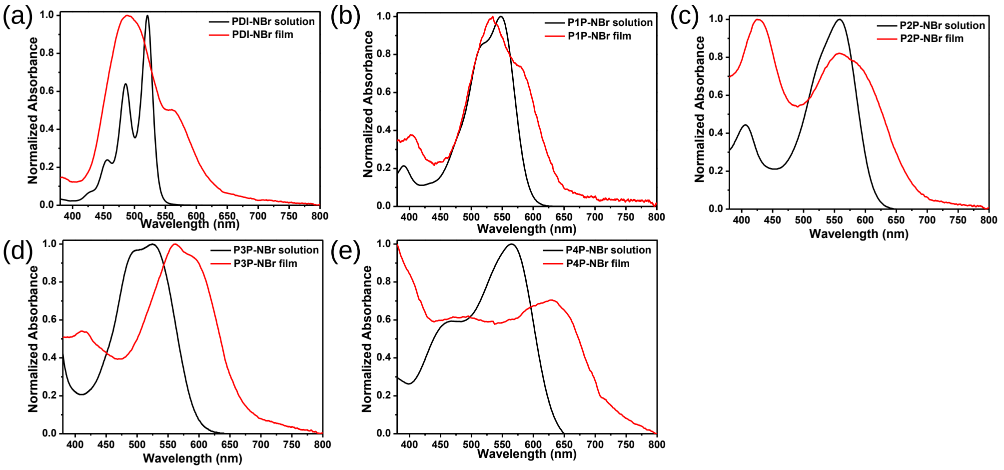

Figure S5. UV-vis absorption spectra of the **PDI-NBr** series in methanol (concentration: 2×10^{-5} mol/L) and film states.

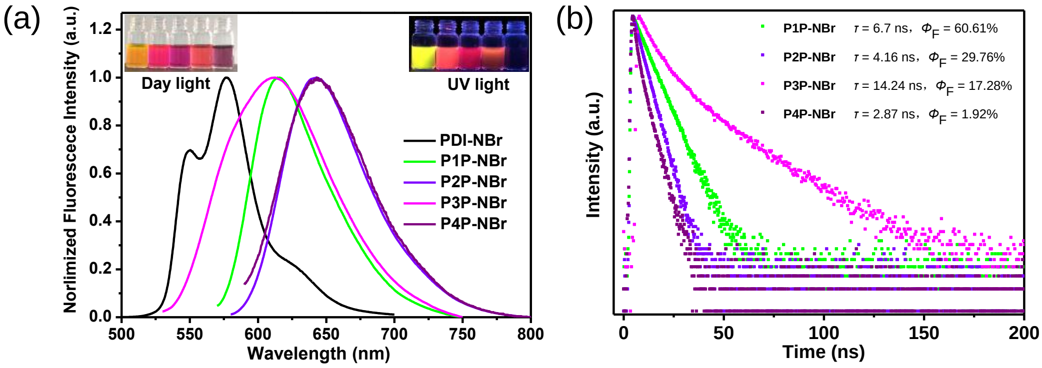

Figure S6. Fluorescence spectra (a) and time-resolved fluorescence decay (b) of the **PDI-NBr** series in methanol (concentration: 2 × 10^{-5} mol/L); inset: photographs of **PDI-NBr**, **P1P-NBr**, **P2P-NBr**, **P3P-NBr** and **P4P-NBr** in methanol under day light and UV light (from left to right).

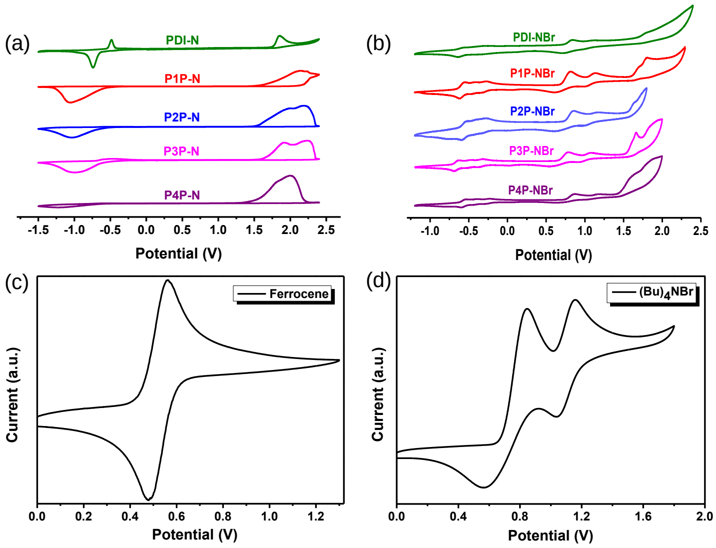

Figure S7. CV curves of the series of **PDI-N** (a) and **PDI-NBr** (b) measured in 0.1 M Bu_4NPF_6 in acetonitrile; CV curves of ferrocene (c) and tetrabutylammonium bromide (d).

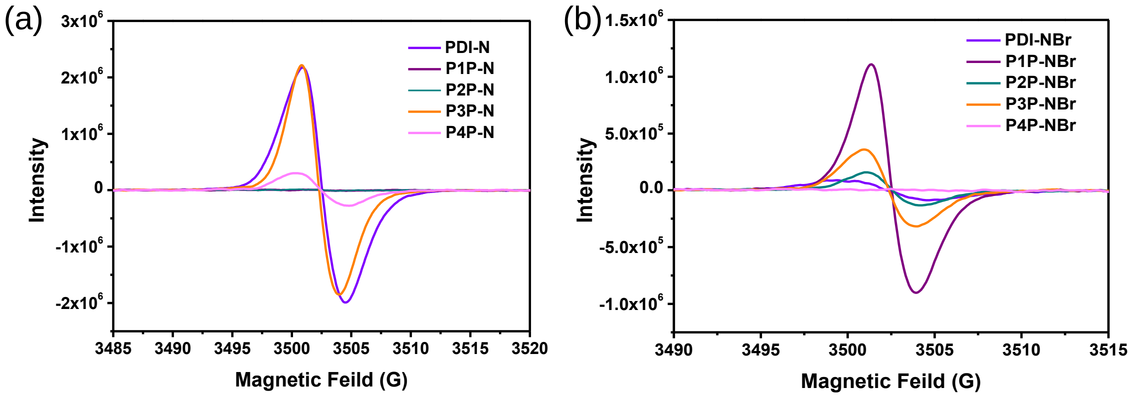

Figure S8. EPR spectra of the series of **PDI-N** (a) and **PDI-NBr** (b) in solid states.

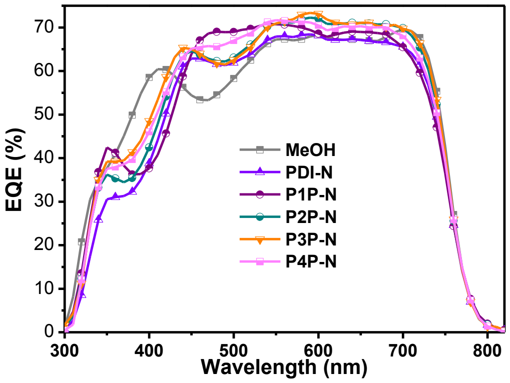

Figure S9. EQE spectra of J71:ITIC-based PSCs with the **PDI-N** series.

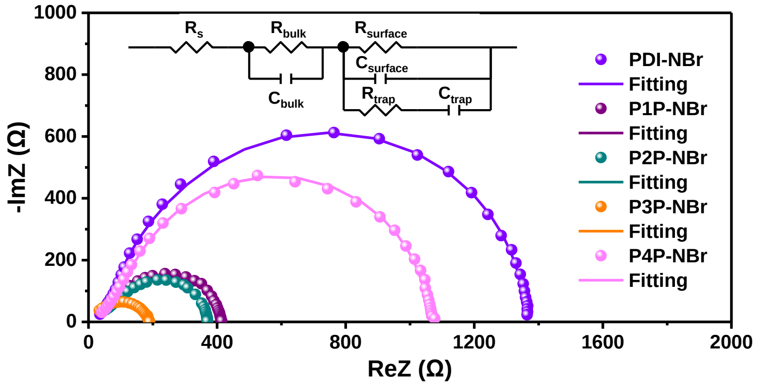

Figure S10. Electrochemical impedance spectroscopies (EIS) of devices with **PDI-NBr** series under the AM 1.5 illumination (Inset: the equivalent circuit used for fitting the impedance data).

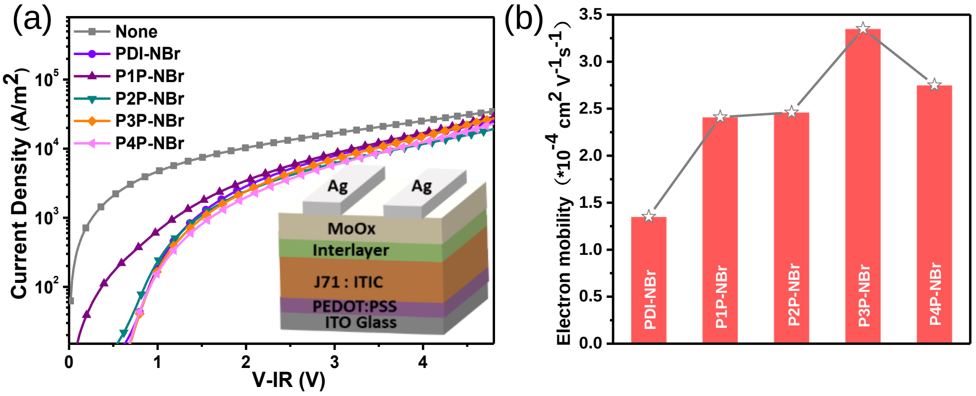

Figure S11. (a) *J-V* curves and the configurations of the hole-only devices with the **PDI-NBr** series; (b) the electron mobility histograms of J71:ITIC-based PSCs with **PDI-NBr** series.

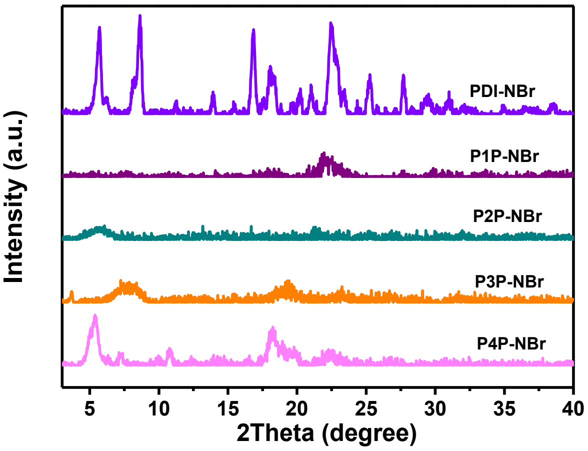

Figure S12. XRD patterns of the **PDI-NBr** series in solid states.

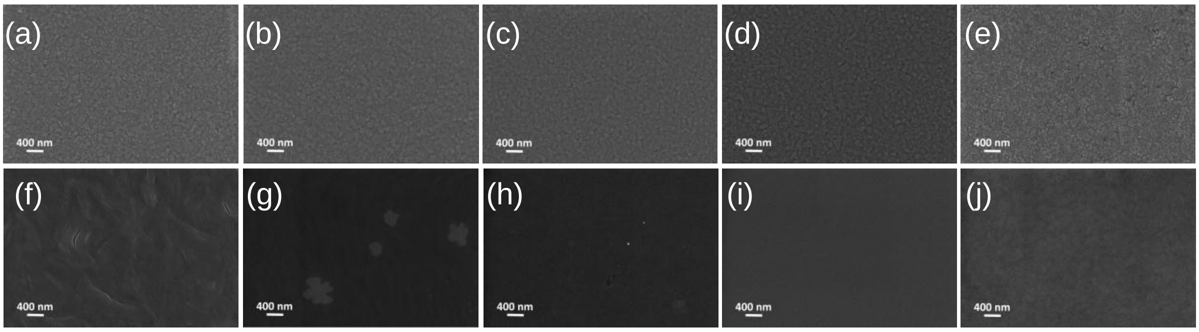

Figure S13. SEM images of the films of **PDI-NBr** (a), **P1P-NBr** (b), **P2P-NBr** (c), **P3P-NBr** (d), **P4P-NBr** (e) on the ITO glass at about 10 nm, and **PDI-NBr** (f), **P1P-NBr** (g), **P2P-NBr** (h), **P3P-NBr** (i) and **P4P-NBr** (j) on the ITO glass at about 30 nm.

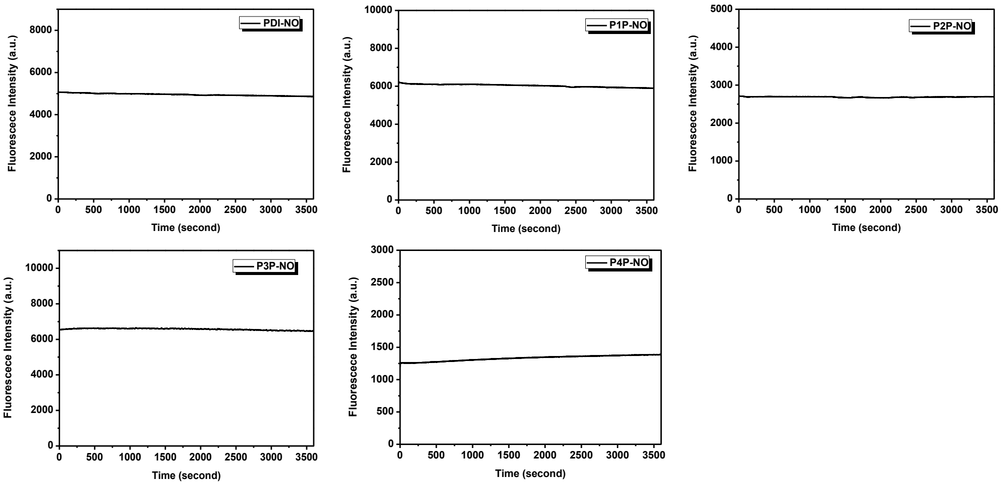

Figure S14. The fluorescence intensity of **PDI-NO** series in methanol solution (concentration: 2 × 10^{-5} mol/L) with increasing scan (0-3600 s) under optimal excitation wavelength irradiation.

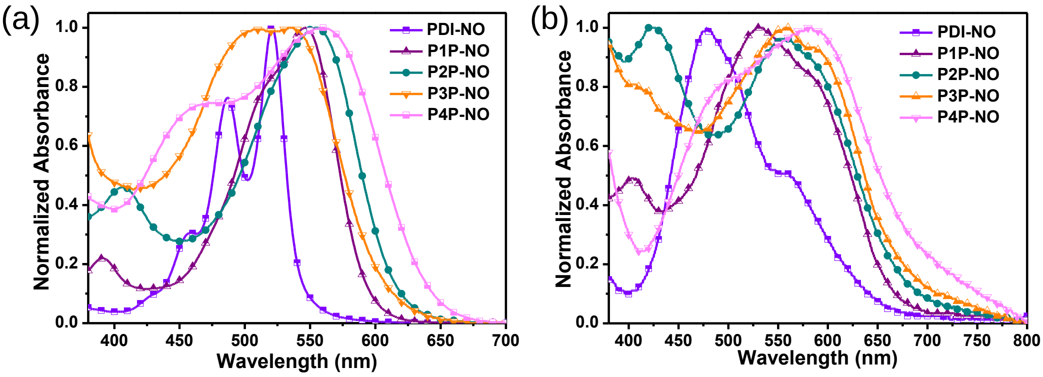

Figure S15. UV-vis absorption spectra of the **PDI-NO** series in methanol (concentration: 2 × 10^{-5} mol/L) (a) and film states (b).

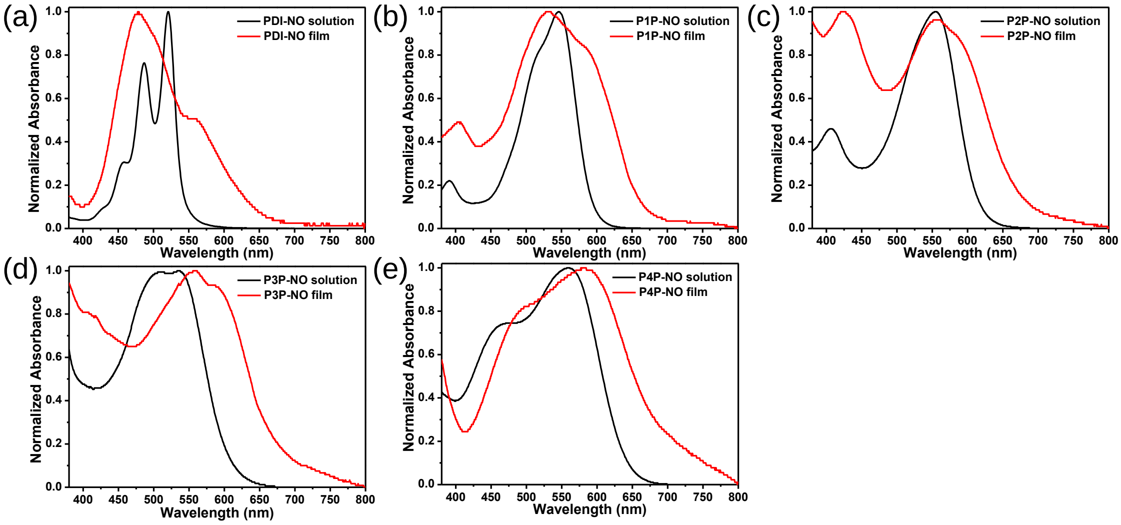

Figure S16. UV-vis absorption spectra of the **PDI-NO** series in methanol (concentration: 2 × 10^{-5} mol/L) and film states.

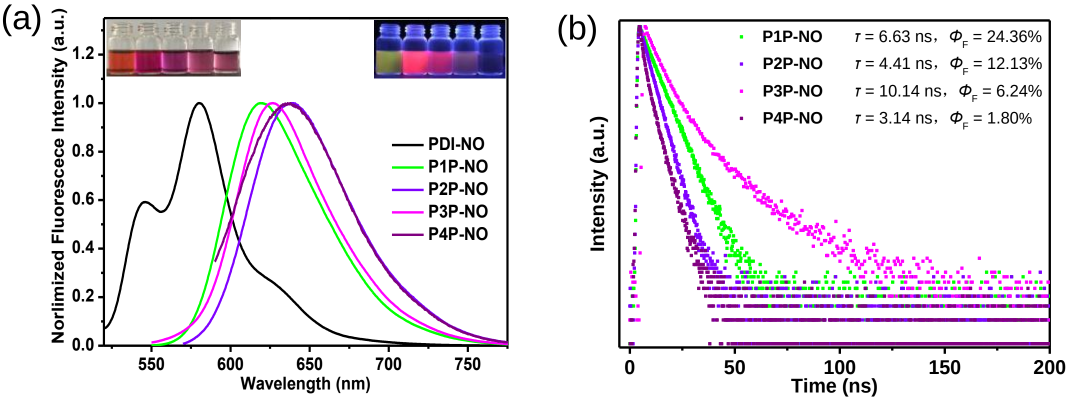

Figure S17. (a) Fluorescence spectra and (b) time-resolved fluorescence decay of the **PDI-NO** series in methanol (concentration: 2 × 10^{-5} mol/L); inset: photographs of **PDI-NO**, **P1P-NO**, **P2P-NO**, **P3P-NO** and **P4P-NO** in methanol under day light and UV light (from left to right).

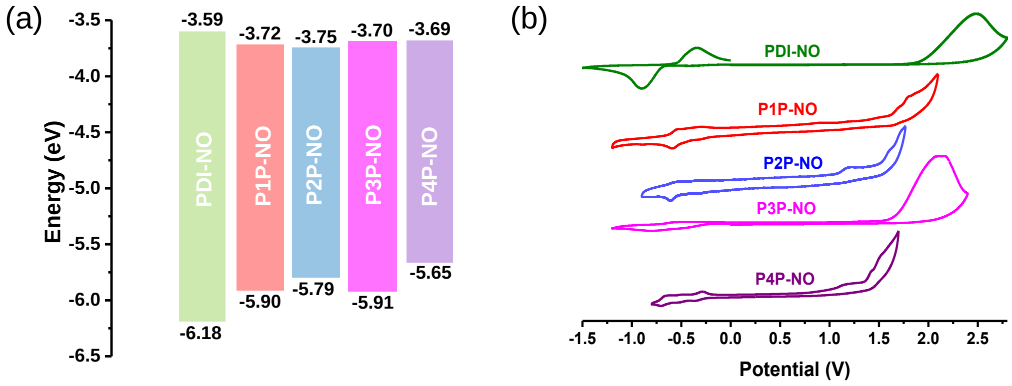

Figure S18. (a) Energy level diagram of the **PDI-NO** series; (b) CV curves of the **PDI-NO** series measured in 0.1 M Bu_4NPF_6 in acetonitrile.

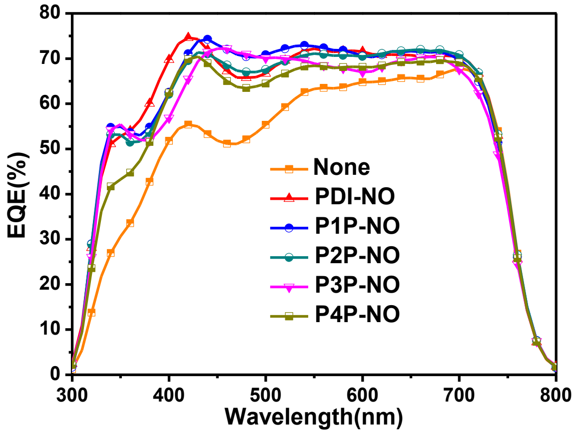

Figure S19. EQE spectra of J71:ITIC-based PSCs with the **PDI-NO** series.

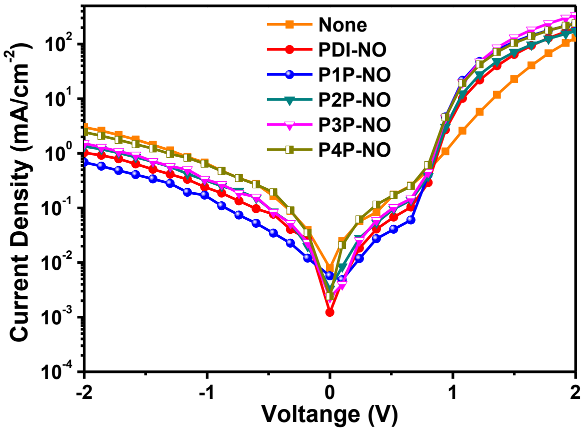

Figure S20. *J-V* curves of J71:ITIC-based PSCs with the **PDI-NO** series in the dark.

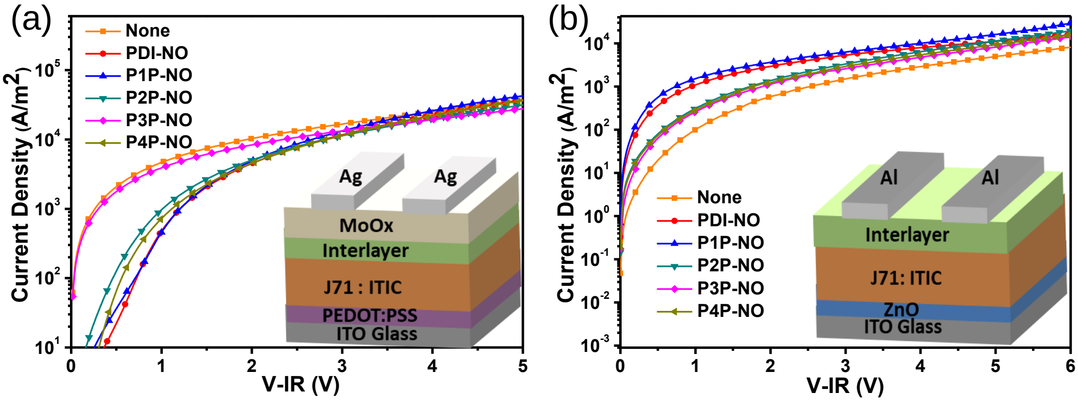

Figure S21. *J-V* curves and the configurations of the hole-only devices (a) and the electron-only devices (b) with the **PDI-NO** series.

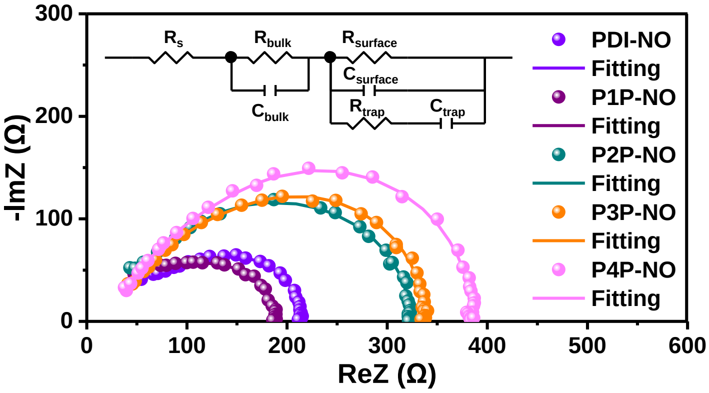

Figure S22. Electrochemical impedance spectroscopies (EIS) of devices with **PDI-NO** series under the AM 1.5 illumination (Inset: the equivalent circuit used for fitting the impedance data).

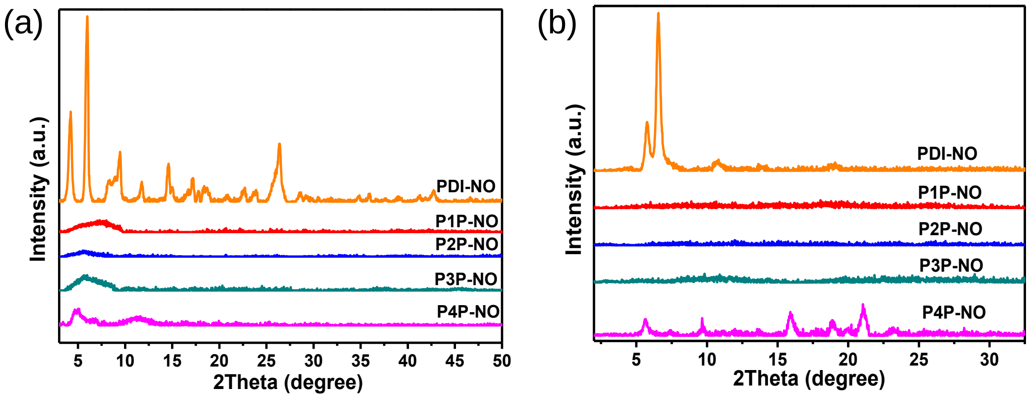

Figure S23. XRD patterns of the **PDI-NO** series in solid states (a), and in film states on a silicon substrates (b).

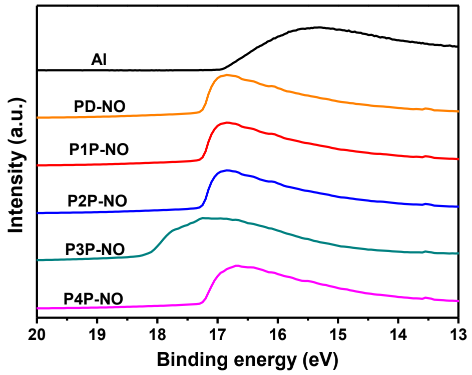

Figure S24. UPS spectra of the aluminum films with the **PDI-NO** series treatments.

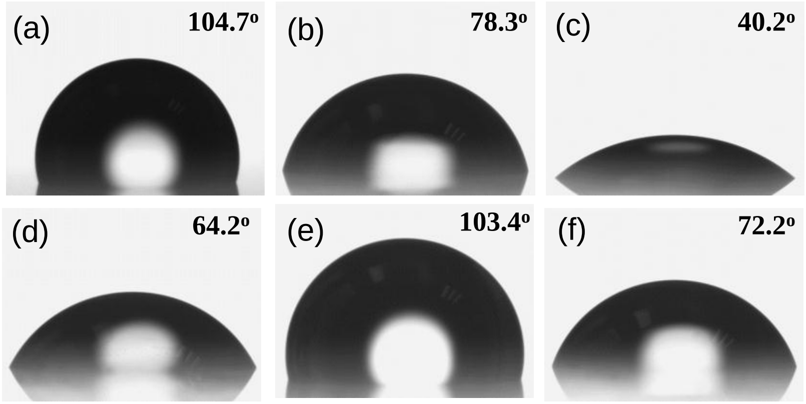

Figure S25. Water contact angle images of (a) MeOH modified, (b) **PDI-NO** modified, (c) **P1P-NO** modified, (d) **P2P-NO** modified, (e) **P3P-NO** modified and (f) **P4P-NO** modified J71:ITIC layers.

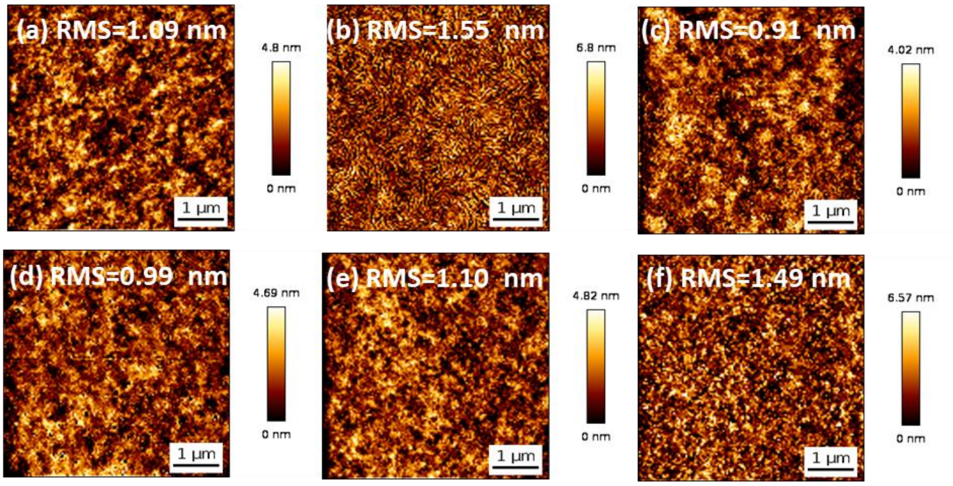

Figure S26. AFM phase images (size: 5 µm× 5 µm) of (a) MeOH modified, (b) **PDI-NO** modified, (c) **P1P-NO** modified, (d) **P2P-NO** modified, (e) **P3P-NO** modified and (f) **P4P-NO** modified J71:ITIC layers.

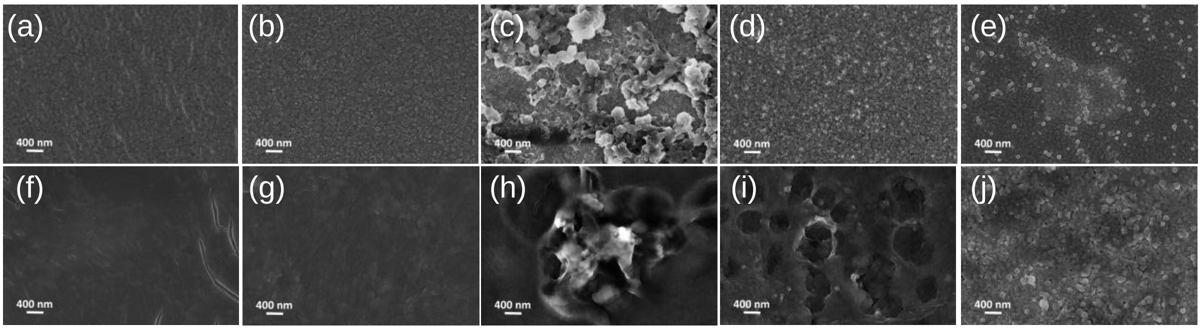

Figure S27. SEM images of the films of **PDI-NO** (a), **P1P-NO** (b), **P2P-NO** (c), **P3P-NO** (d), **P4P-NO** (e) on the ITO glass at about 10 nm, and **PDI-NO** (f), **P1P-NO** (g), **P2P-NO** (h), **P3P-NO** (i) and **P4P-NO** (j) on the ITO glass at about 30 nm.

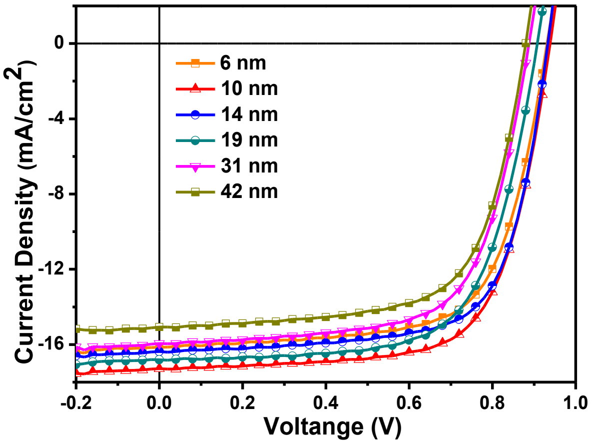

Figure S28. *J-V* curves of the PSCs based on J71:ITIC with **P1P-NO** in various thicknesses.

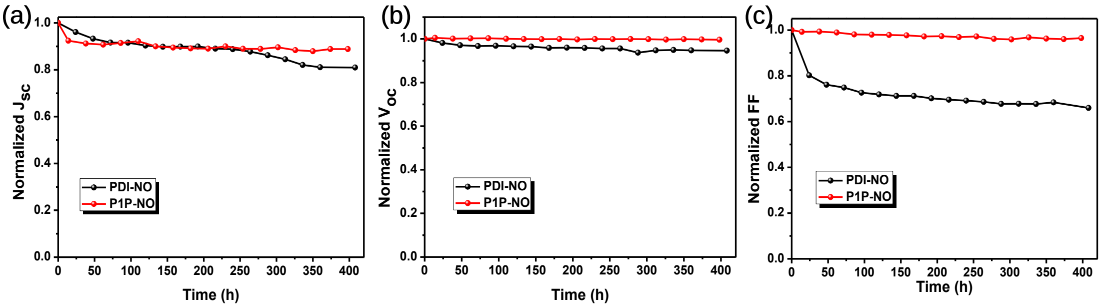

Figure S29. The curves of normalized J_{sc} (a), V_{oc} (b) and *FF* (c) *versus* time of devices with **PDI-NO** and **P1P-NO** in an atmosphere of nitrogen without encapsulation.

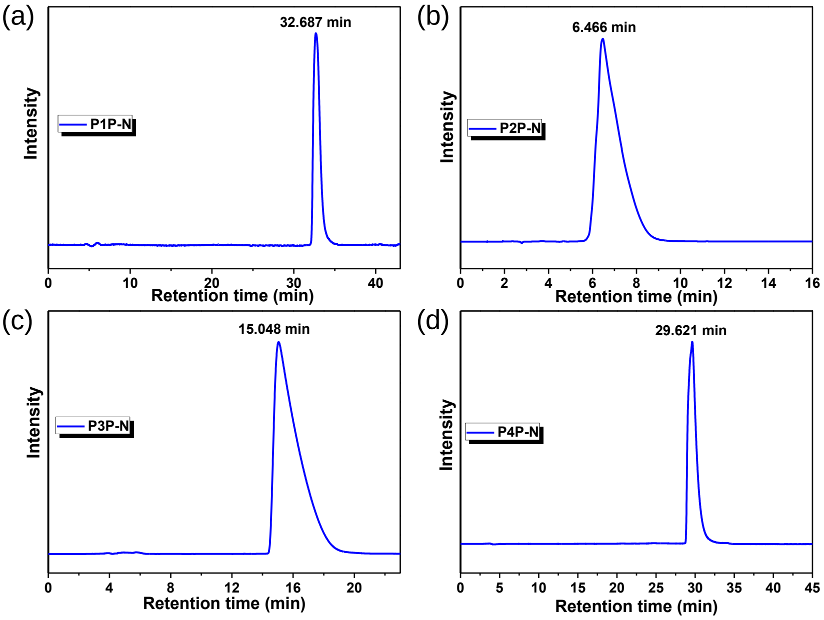

Figure S30. HPLC curves for (a) **P1P-N**, (b) **P2P-N**, (c) **P3P-N** and (d) **P4P-N**.

Table S1. The optimal geometrics of the **PDI-NBr** series were calculated by the Gaussian 09 program at the B3LYP/6-31G* level.

CILs	PDI-NBr	P1P-NBr	P2P-NBr	P3P-NBr	P4P-NBr
Optimized geometry	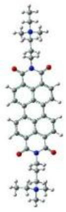	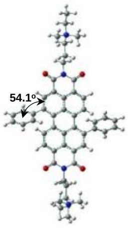	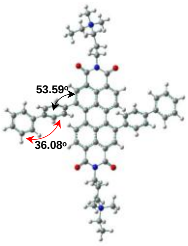	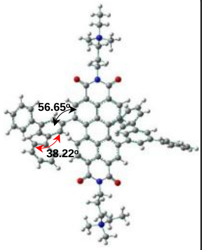	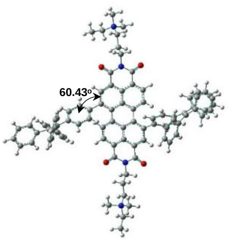

Table S2. The fitting results of the Nyquist plots of devices with **PDI-NBr** series.

CILs	R_{surface} (Ω cm^2)
PDI-NBr	1220
P1P-NBr	307.9
P2P-NBr	290.1
P3P-NBr	75.52
P4P-NBr	961.8

Table S3. The mobility results of **PDI-NBr** series.

CILs	μ_e [cm^2 V^{-1} s^{-1}]	μ_h [cm^2 V^{-1} s^{-1}]	μ_e/μ_h
none	7.53E-06	7.62E-04	0.01
PDI-NBr	1.35E-04	7.02E-05	1.92
P1P-NBr	2.41E-04	1.71E-04	1.41
P2P-NBr	2.46E-04	1.48E-04	1.66
P3P-NBr	3.35E-04	1.97E-04	1.70
P4P-NBr	2.75E-04	1.21E-04	2.27

Table S4. UV-vis absorption and electrochemical properties of the **PDI-NO** series.

Compounds	λ_{abs} (nm) in solution	λ_{abs}(nm) in film	λ_{onset} [a] (nm)	$E_{g(opt)}$ [b] (eV)	E_{LUMO} [c] (eV)	E_{HOMO} [d] (eV)	E_g [e] (eV)
PDI-NO	521	480	645	1.92	-3.59	-6.18	2.59
P1P-NO	547	530	663	1.87	-3.72	-5.90	2.18
P2P-NO	553	554	672	1.85	-3.75	-5.79	2.04
P3P-NO	535	559	685	1.81	-3.70	-5.91	2.21
P4P-NO	560	584	711	1.74	-3.69	-5.65	1.96

[a] Film; [b] optical band gap calculated from film absorption as $E_g = 1240/\lambda_{onset}$; [c] calculated from the onset reduction potentials of the compounds; [d] calculated from the onset oxidation potentials of the compounds; [e] $E_g = E_{LUMO} - E_{HOMO}$.

Table S5. The HOMO/LUMO distribution and optimal geometrics of the **PDI-NO** series were calculated by the Gaussian 09 program at the B3LYP/6-31G* level.

	PDI-NO	**P1P-NO**	**P2P-NO**	**P3P-NO**	**P4P-NO**
Optimized geometry	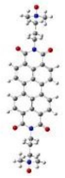		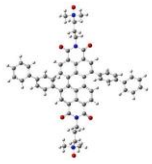	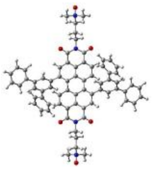	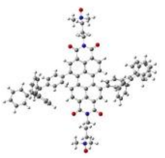
HOMO	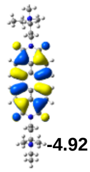	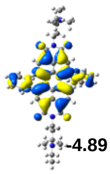	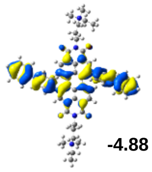	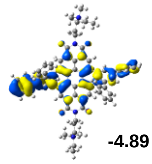	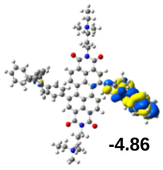
LUMO	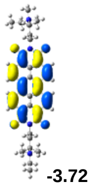	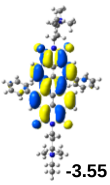	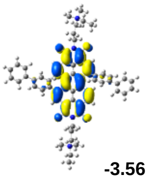	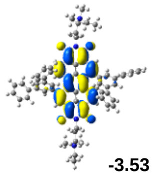	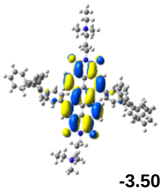

Table S6. The mobility results of **PDI-NO** series.

CILs	μ_e [cm^2 V^{-1} s^{-1}]	μ_h [cm^2 V^{-1} s^{-1}]	μ_e/μ_h
none	7.53E-06	7.62E-04	0.01
PDI-NO	1.21E-04	4.73E-04	0.26
P1P-NO	1.60E-04	6.55E-04	0.24
P2P-NO	1.59E-05	4.27E-04	0.04
P3P-NO	8.02E-06	3.89E-04	0.02
P4P-NO	1.32E-05	2.12E-04	0.06

Table S7. The fitting results of the Nyquist plots of devices with **PDI-NO** series.

CILs	$R_{surface}$ (Ω cm^2)
PDI-NO	149
P1P-NO	128
P2P-NO	172.4
P3P-NO	240.4
P4P-NO	288.6

Table S8. Device parameters of the PSCs based on J71:ITIC with **P1P-NO** in various thicknesses.

Interlayer Thickness (nm)	V_{oc} (V)	J_{sc} (mA/cm^2)	*FF* (%)	Average PCE (%)	PCE (%)
6	0.931	16.15	67.78	9.93±0.27	10.20
9	0.940	17.47	70.29	11.23±0.19	11.56
14	0.933	16.37	69.63	10.45±0.13	10.64
19	0.908	16.80	66.96	10.04±0.19	10.22
31	0.887	15.95	66.73	9.27±0.17	9.44
42	0.880	15.51	66.87	8.67±0.15	8.88

*Average values with standard deviation were obtained from 8 devices.

4. NMR Spectra

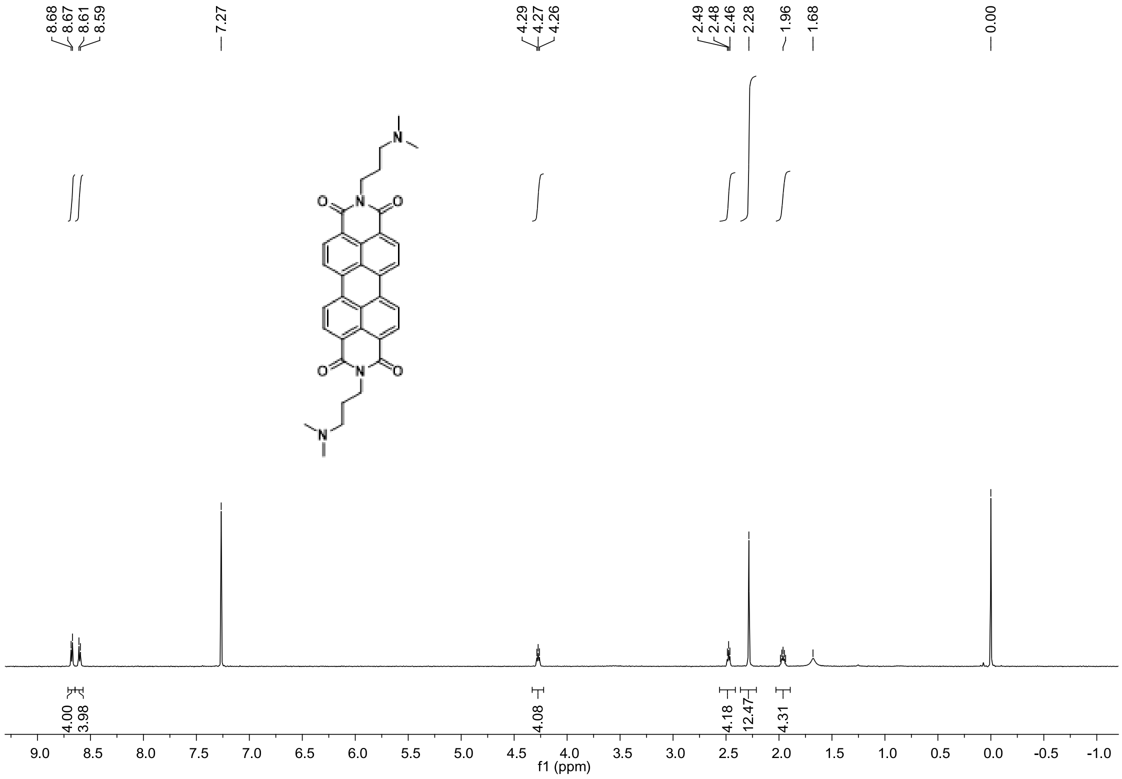

Figure S31. ^{1}H NMR spectrum of compound **1** in CDCl$_3$.

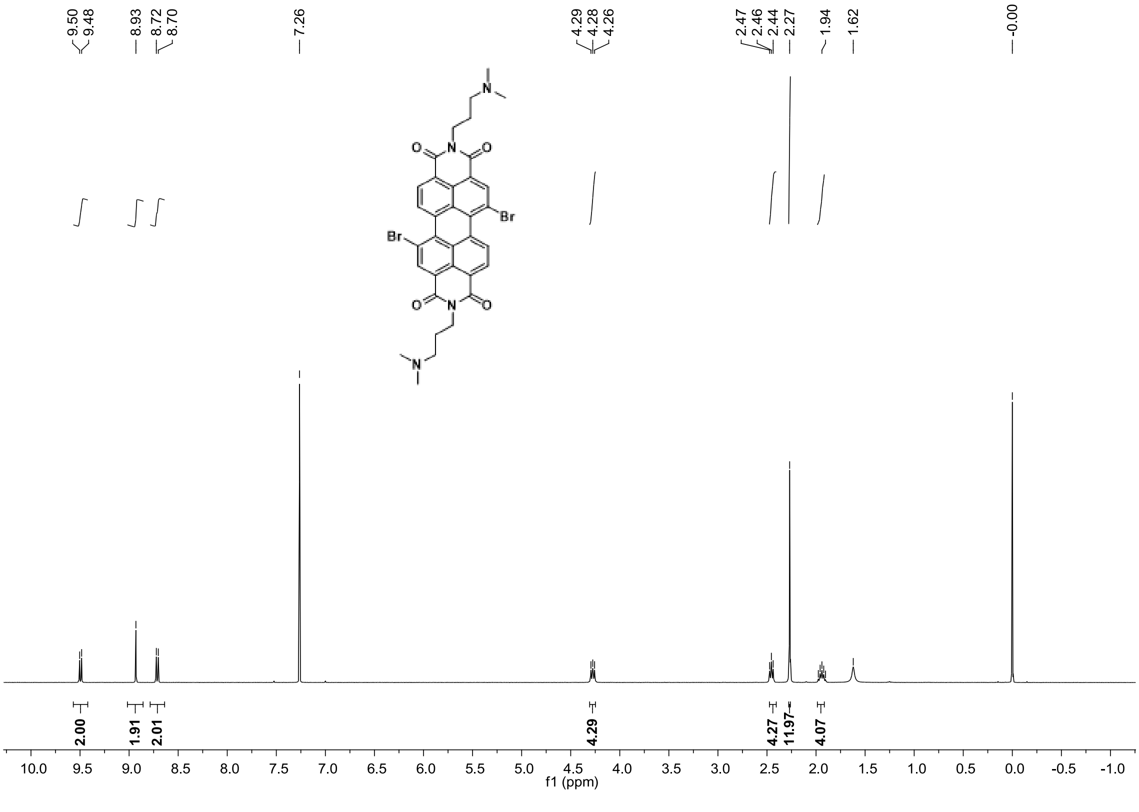

Figure S32. ^{1}H NMR spectrum of compound **3** in CDCl$_3$.

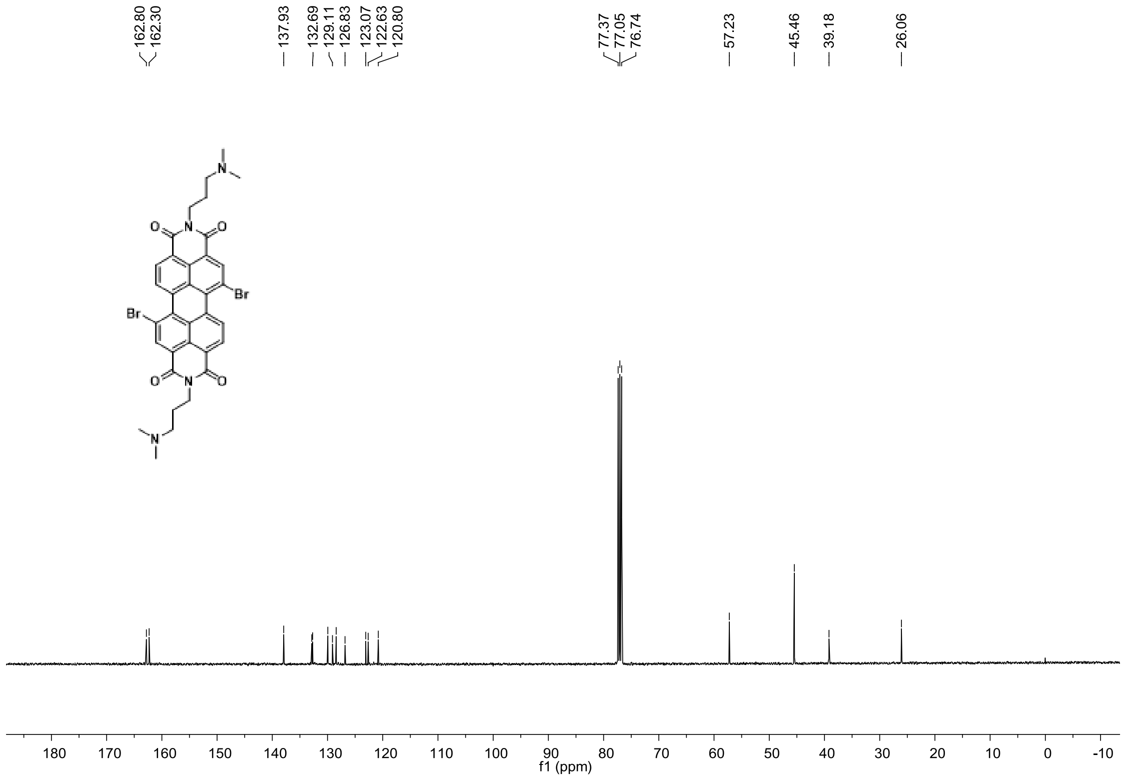

Figure S33. ^{13}C NMR spectrum of compound **3** in CDCl$_3$.

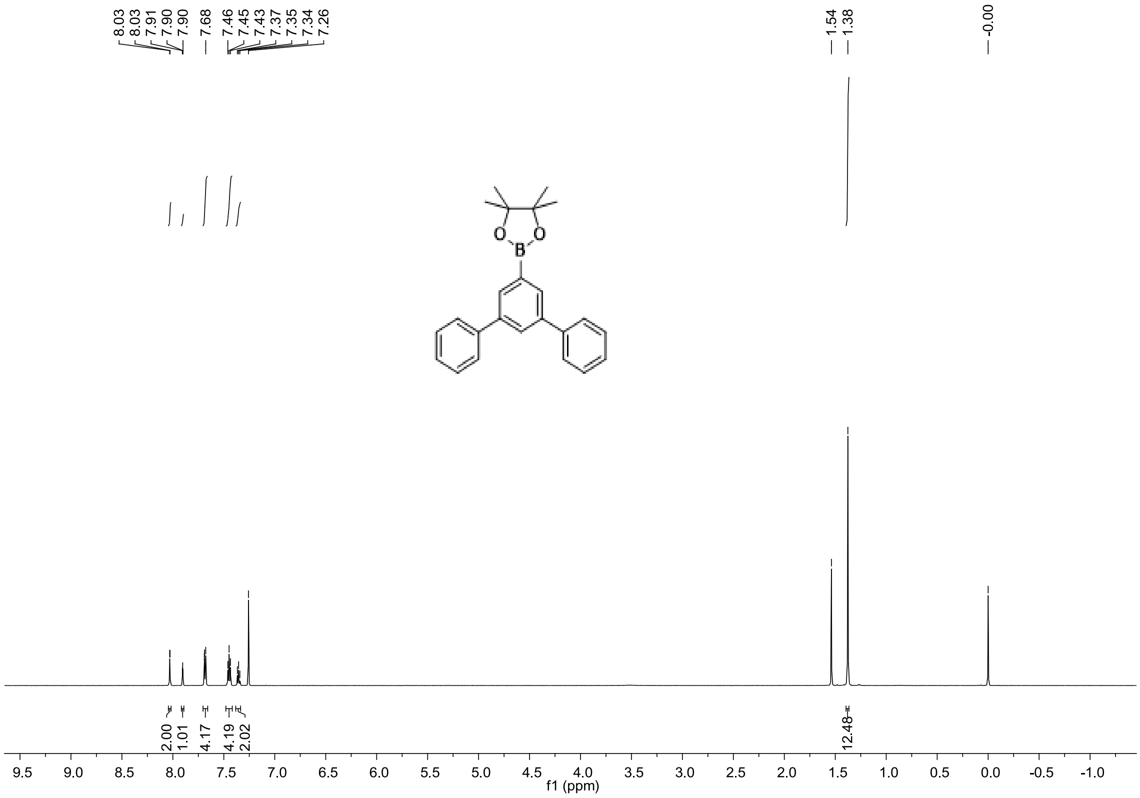

Figure S34. ^{1}H NMR spectrum of compound **4** in CDCl$_3$.

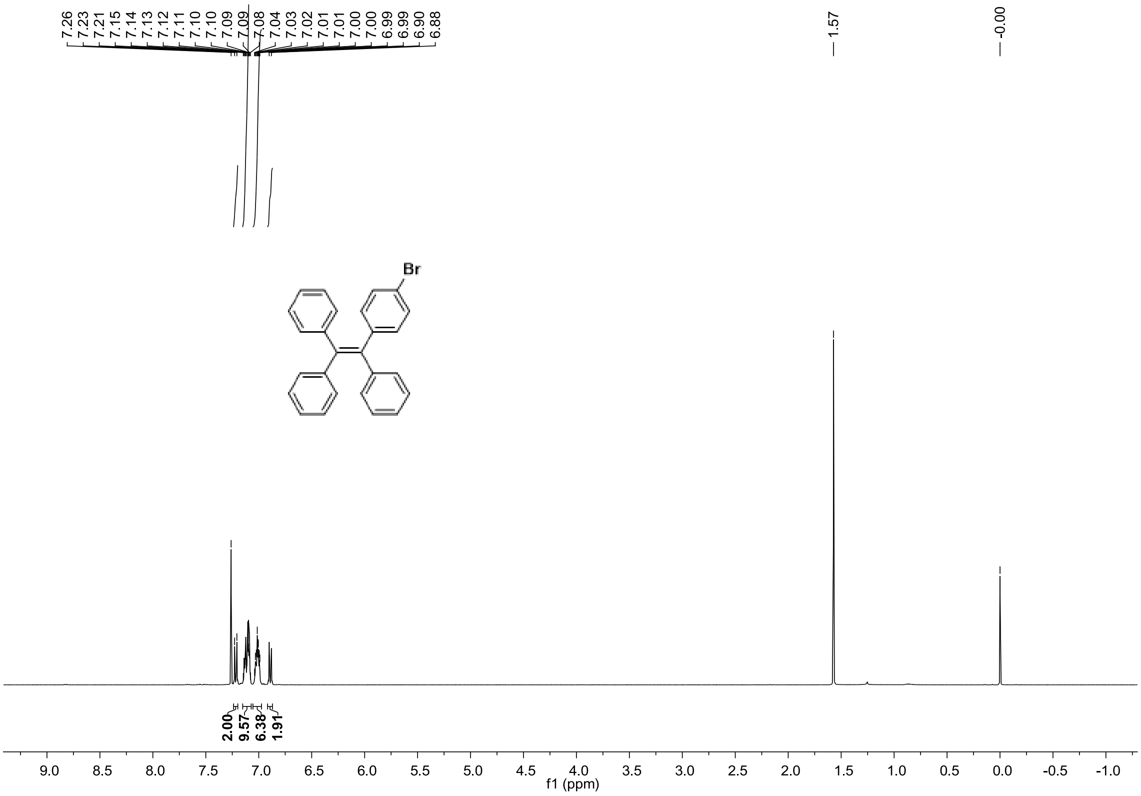

Figure S35. ^{1}H NMR spectrum of compound **5** in $CDCl_3$.

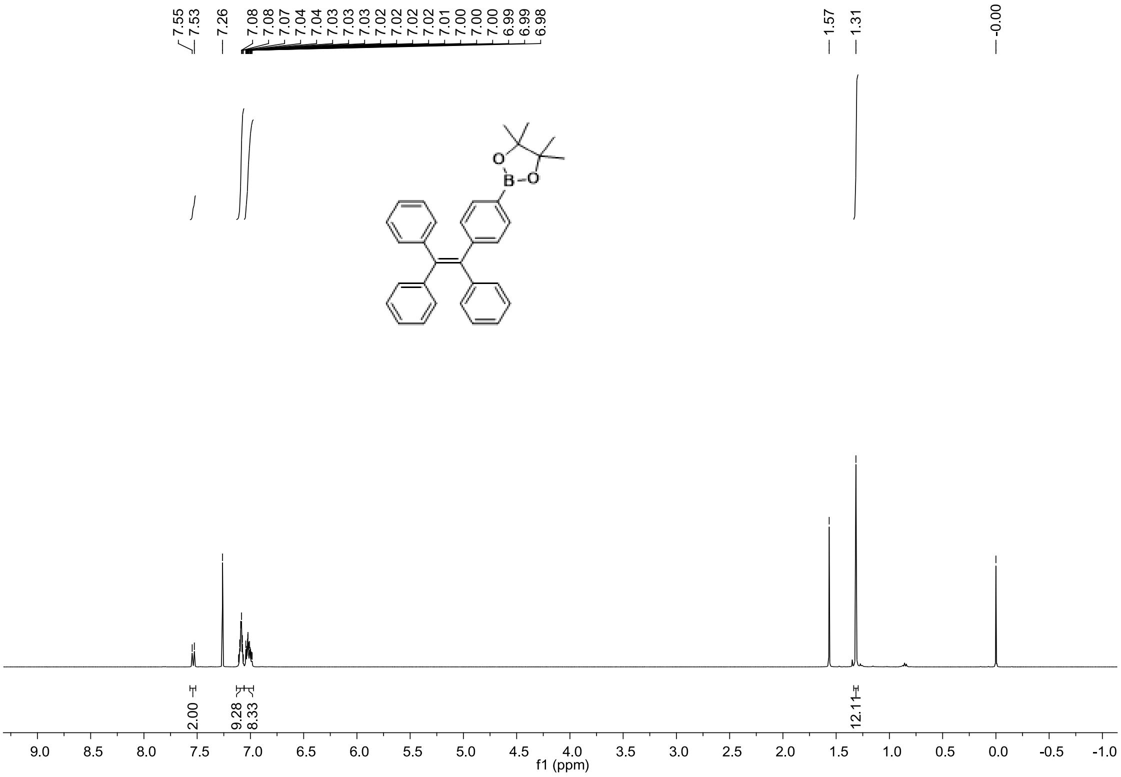

Figure S36. ^{1}H NMR spectrum of compound **6** in $CDCl_3$.

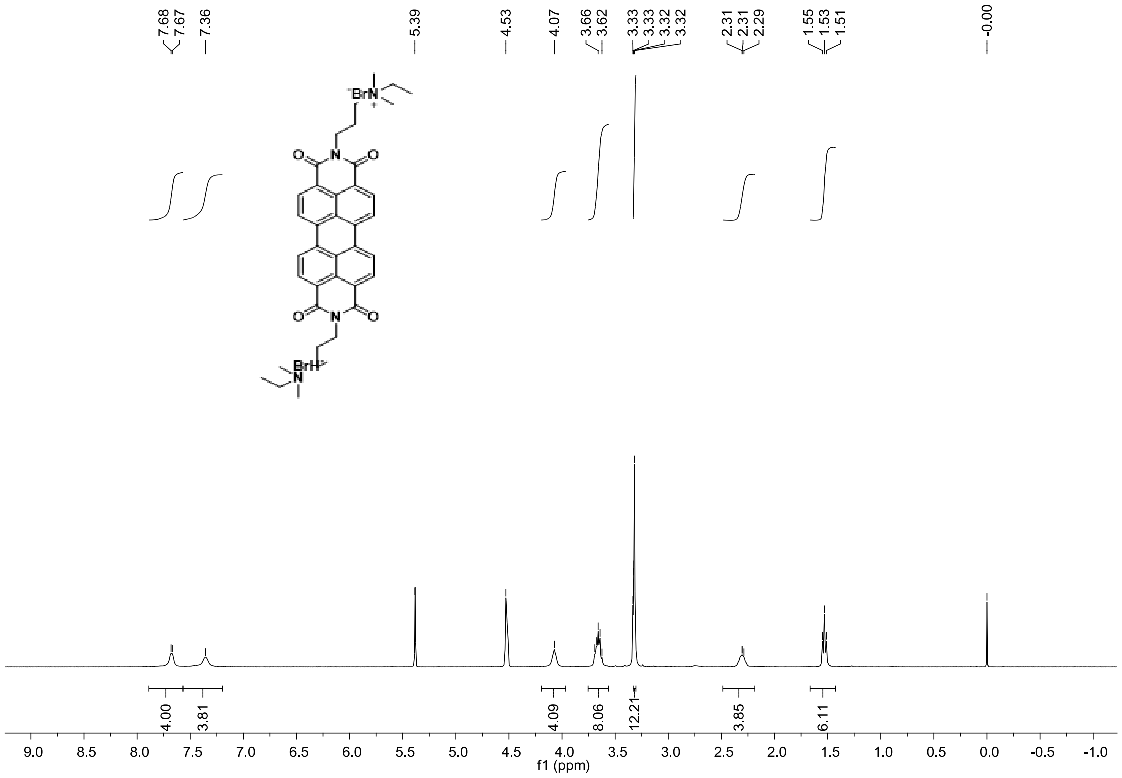

Figure S37. ^{1}H NMR spectrum of compound **7** in the mixture solvent of CD_2Cl_2 and CD_3OD.

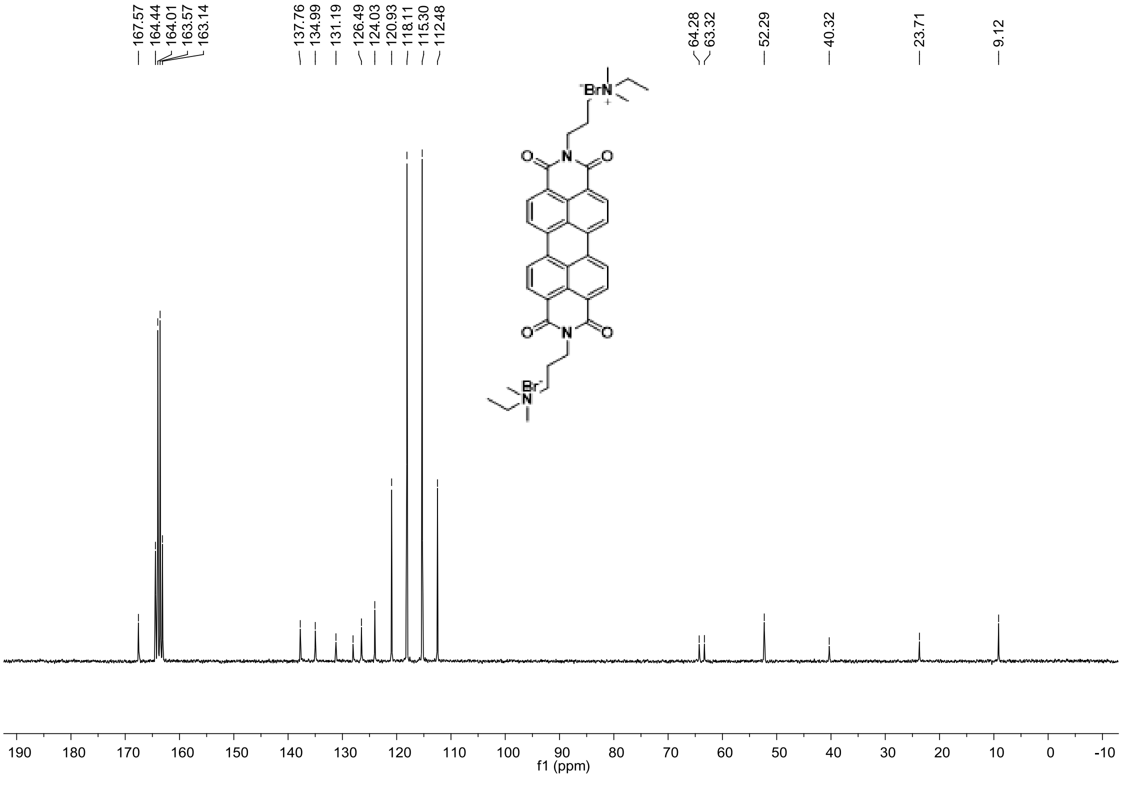

Figure S38. ^{13}C NMR spectrum of compound **7** in CF_3COOD.

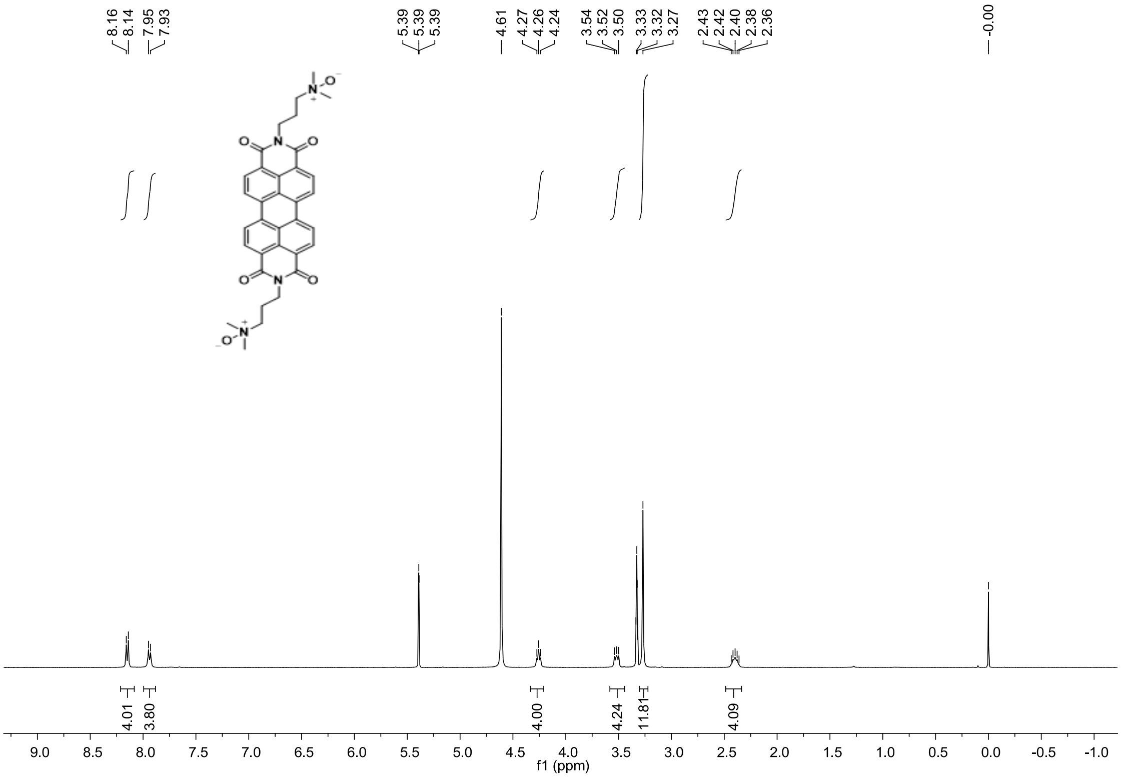

Figure S39. ^{1}H NMR spectrum of compound **8** in the mixture solvent of CD_2Cl_2 and CD_3OD.

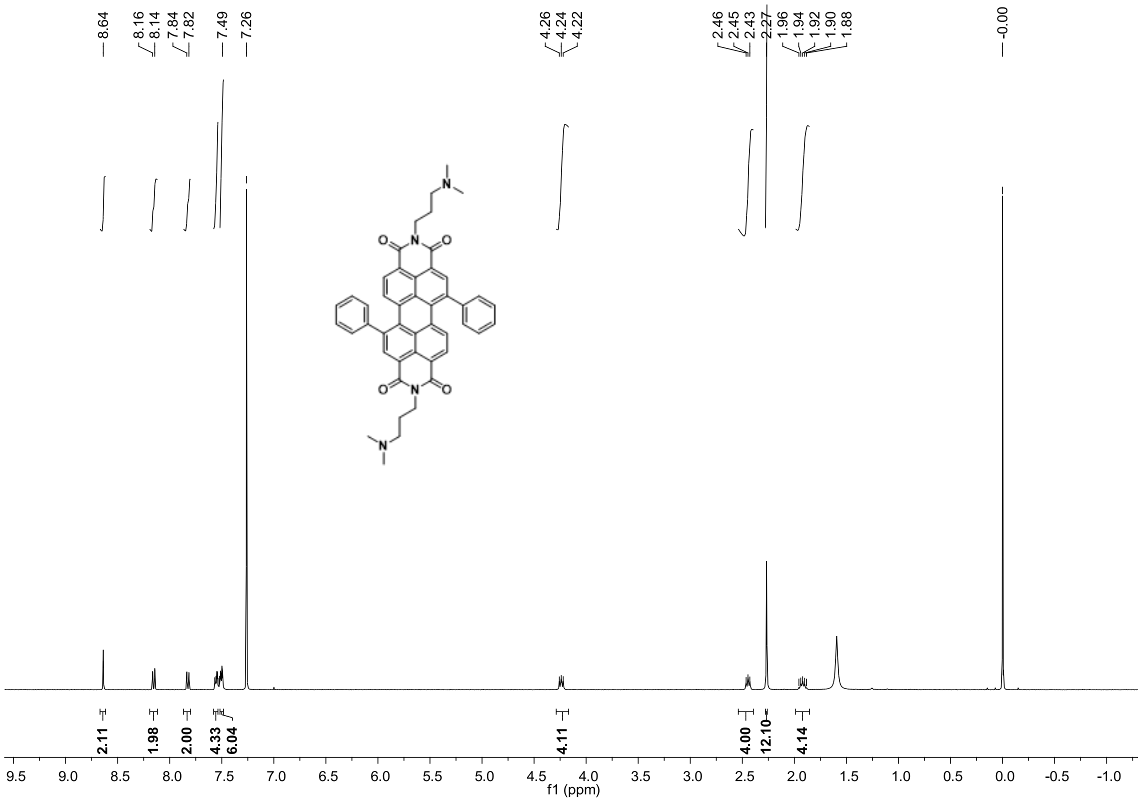

Figure S40. ^{1}H NMR spectrum of compound **9** in CDCl$_3$.

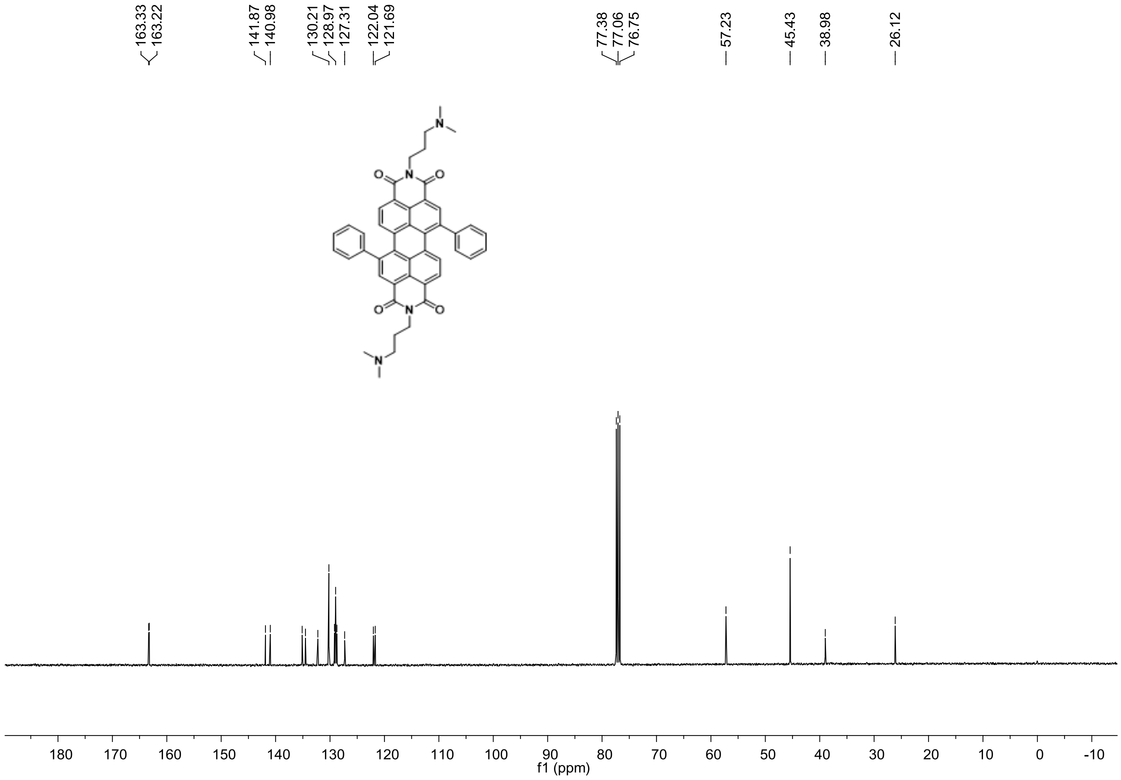

Figure S41. ^{13}C NMR spectrum of compound **9** in CDCl$_3$.

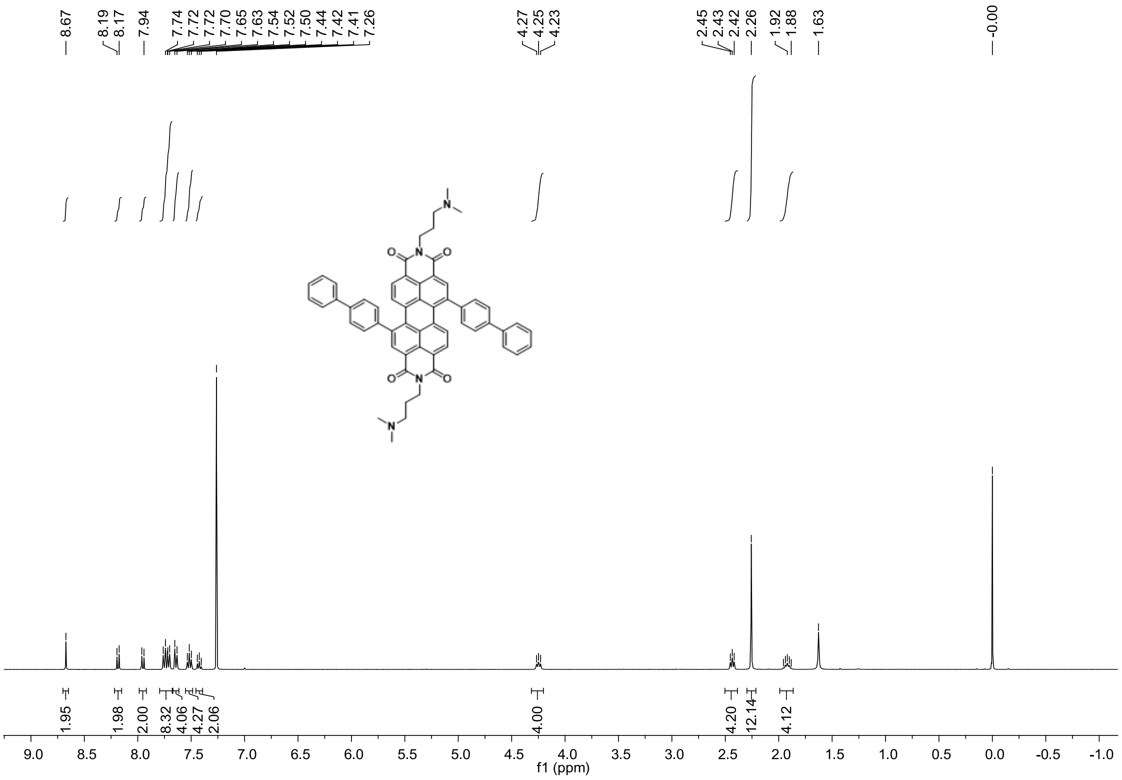

Figure S42. ^{1}H NMR spectrum of compound **10** in CDCl$_3$.

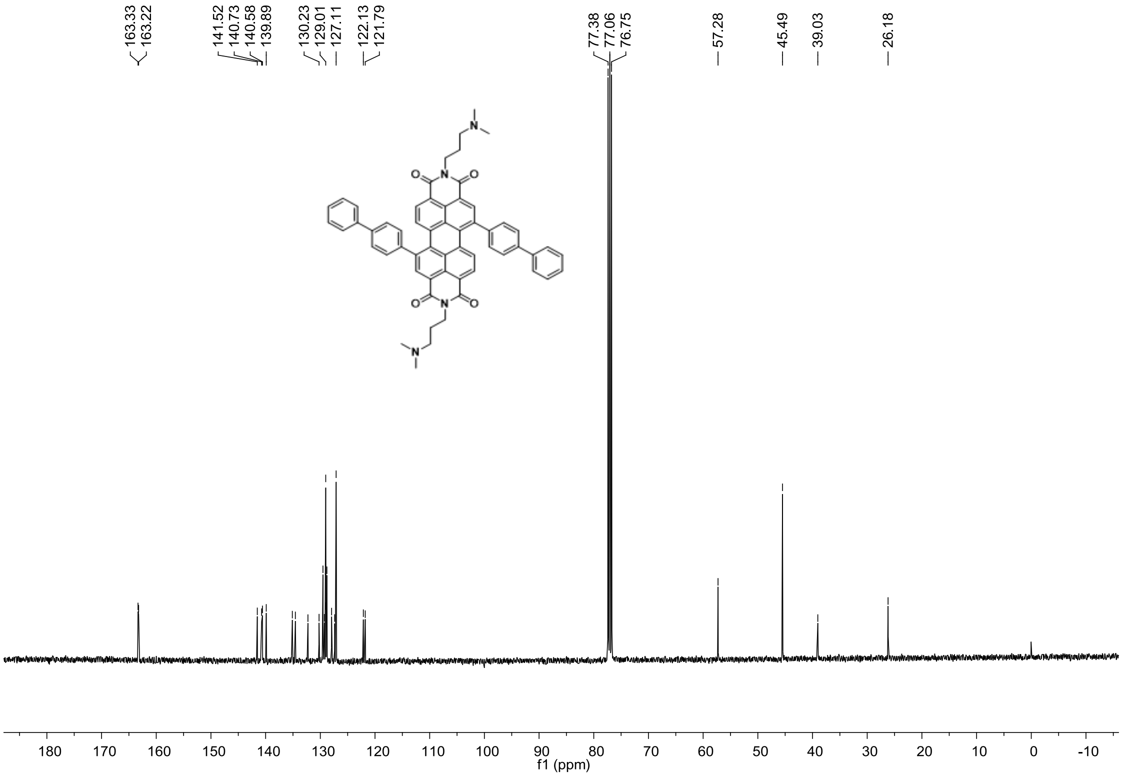

Figure S43. ^{13}C NMR spectrum of compound **10** in CDCl$_3$.

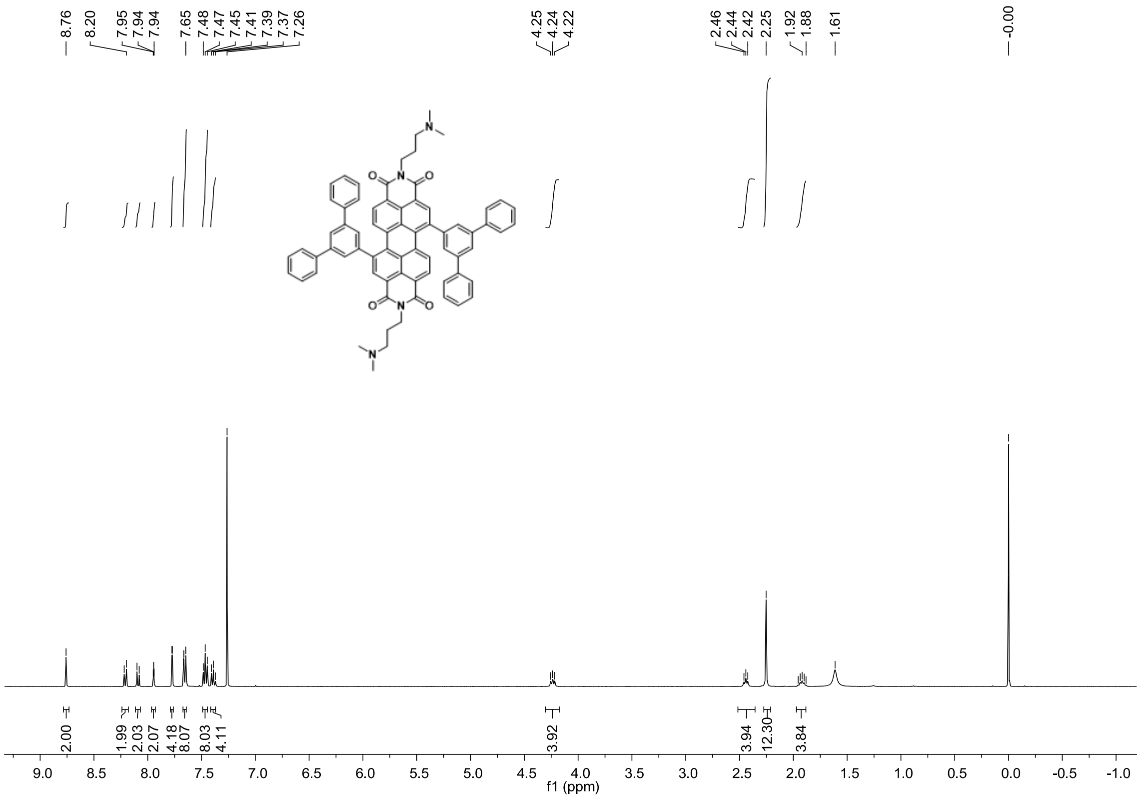

Figure S44. ^{1}H NMR spectrum of compound **11** in $CDCl_3$.

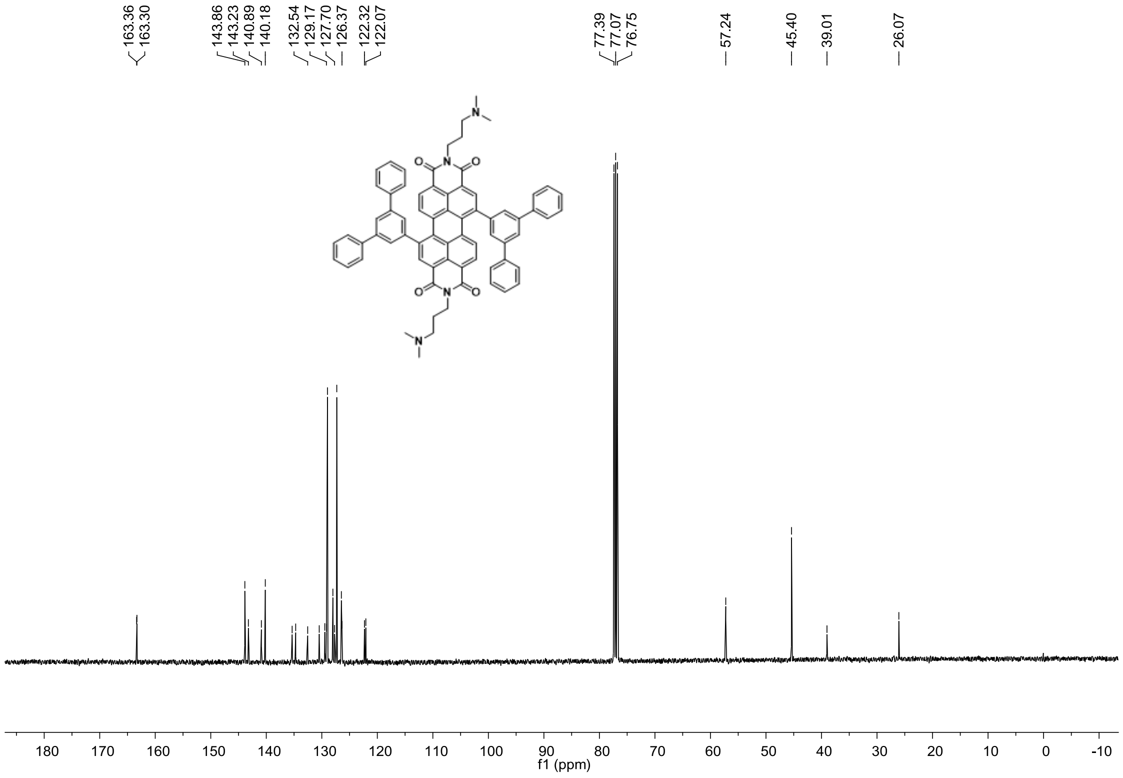

Figure S45. ^{13}C NMR spectrum of compound **11** in $CDCl_3$.

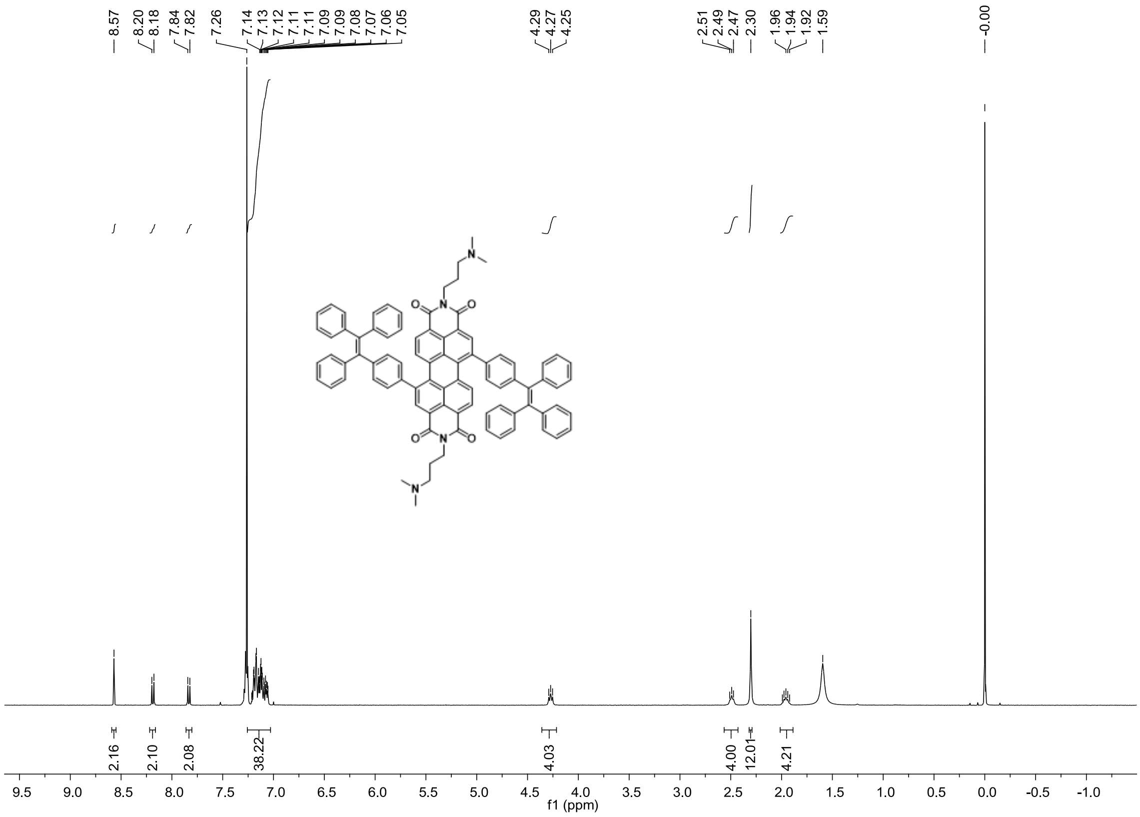

Figure S46. ^{1}H NMR spectrum of compound **12** in CDCl$_3$.

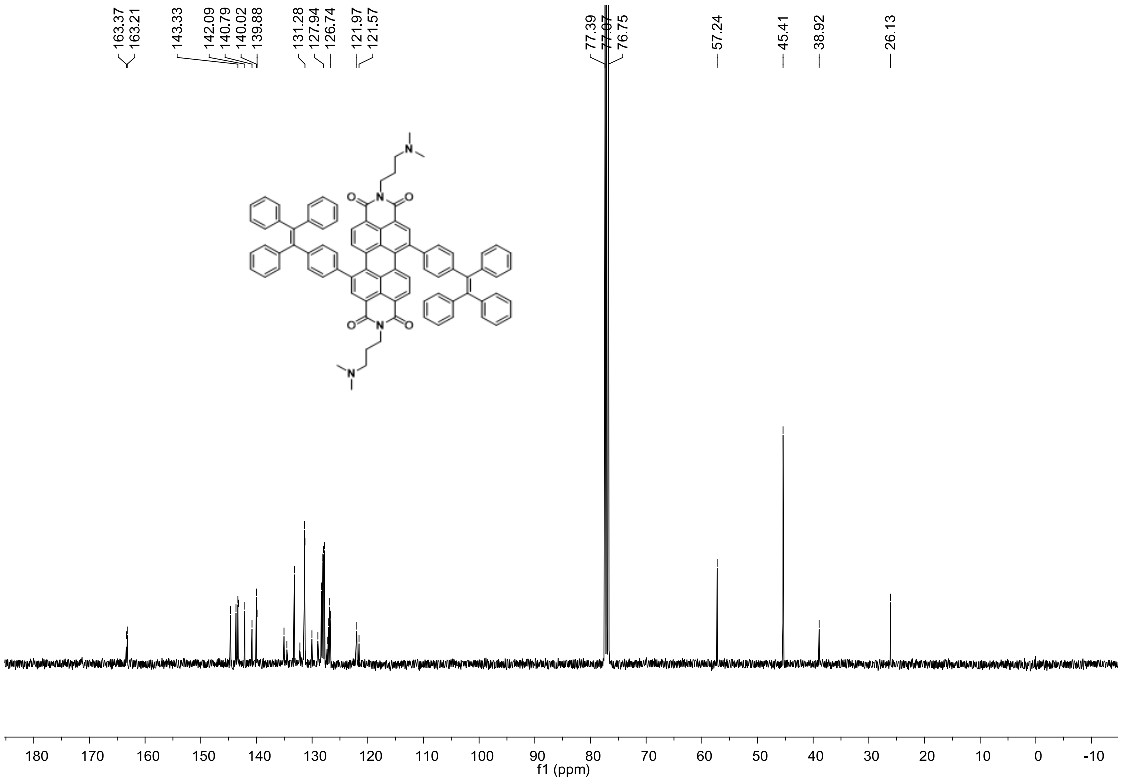

Figure S47. ^{13}C NMR spectrum of compound **12** in CDCl$_3$.

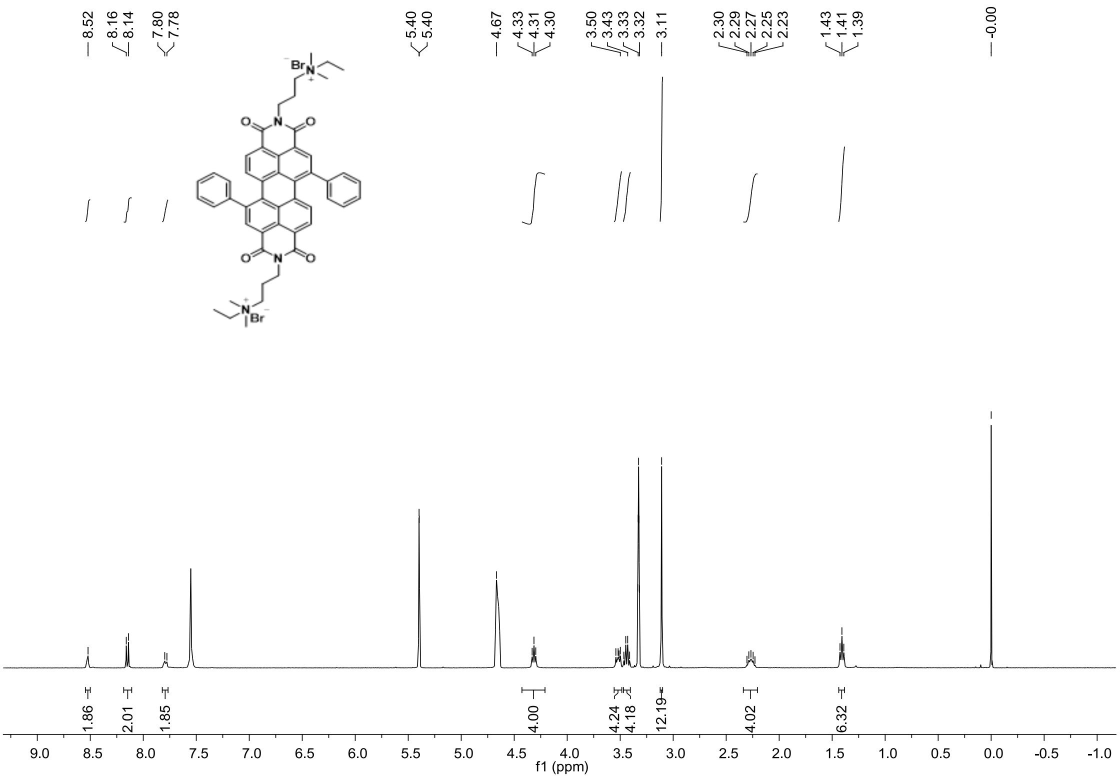

Figure S48. ^{1}H NMR spectrum of compound **13** in the mixture solvent of CD_2Cl_2 and CD_3OD.

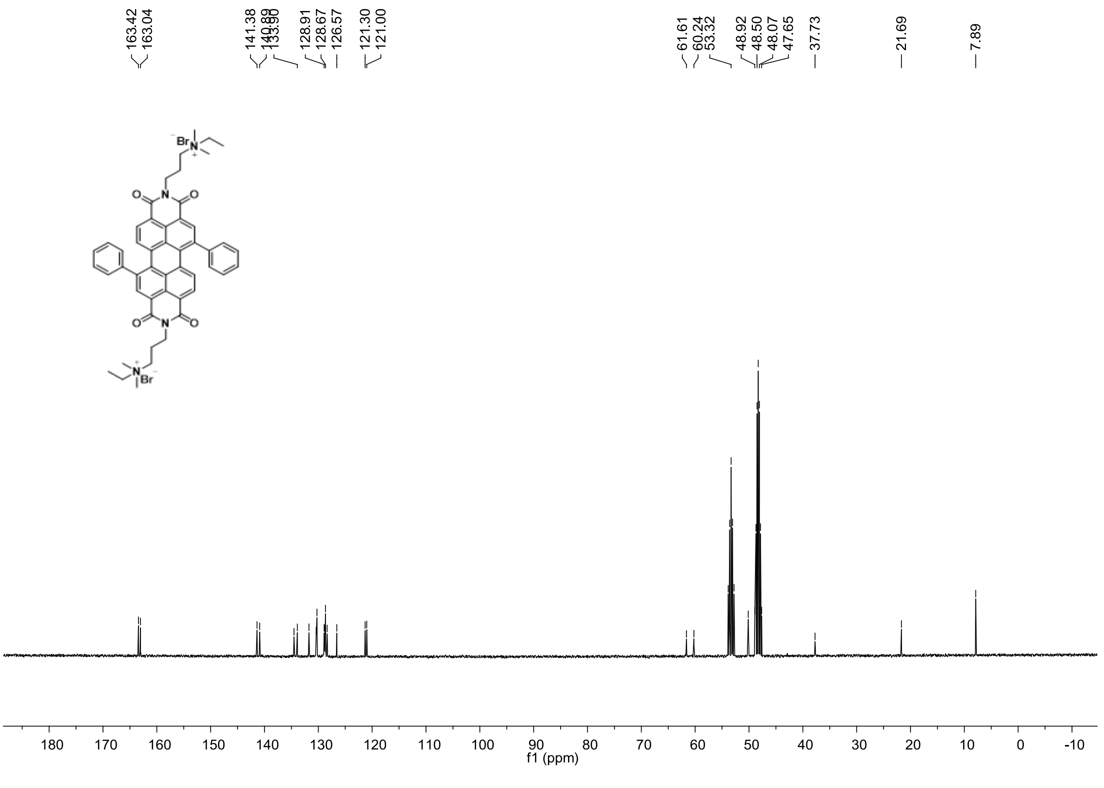

Figure S49. ^{13}C NMR spectrum of compound **13** in the mixture solvent of CD_2Cl_2 and CD_3OD.

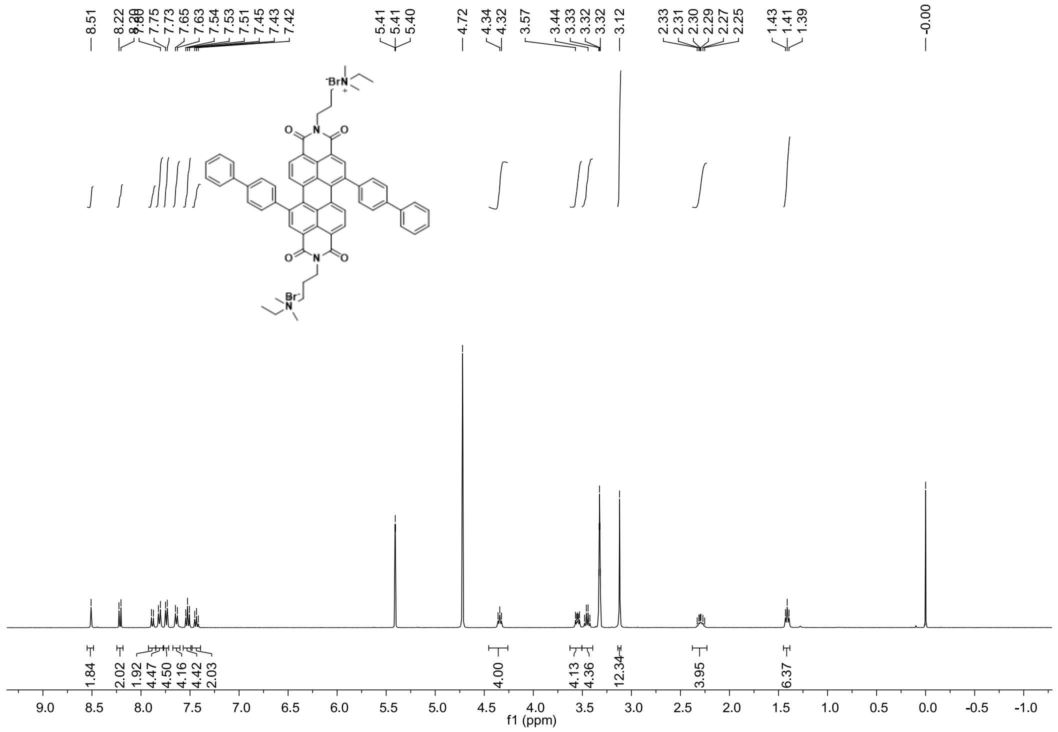

Figure S50. ^{1}H NMR spectrum of compound **14** in the mixture solvent of CD_2Cl_2 and CD_3OD.

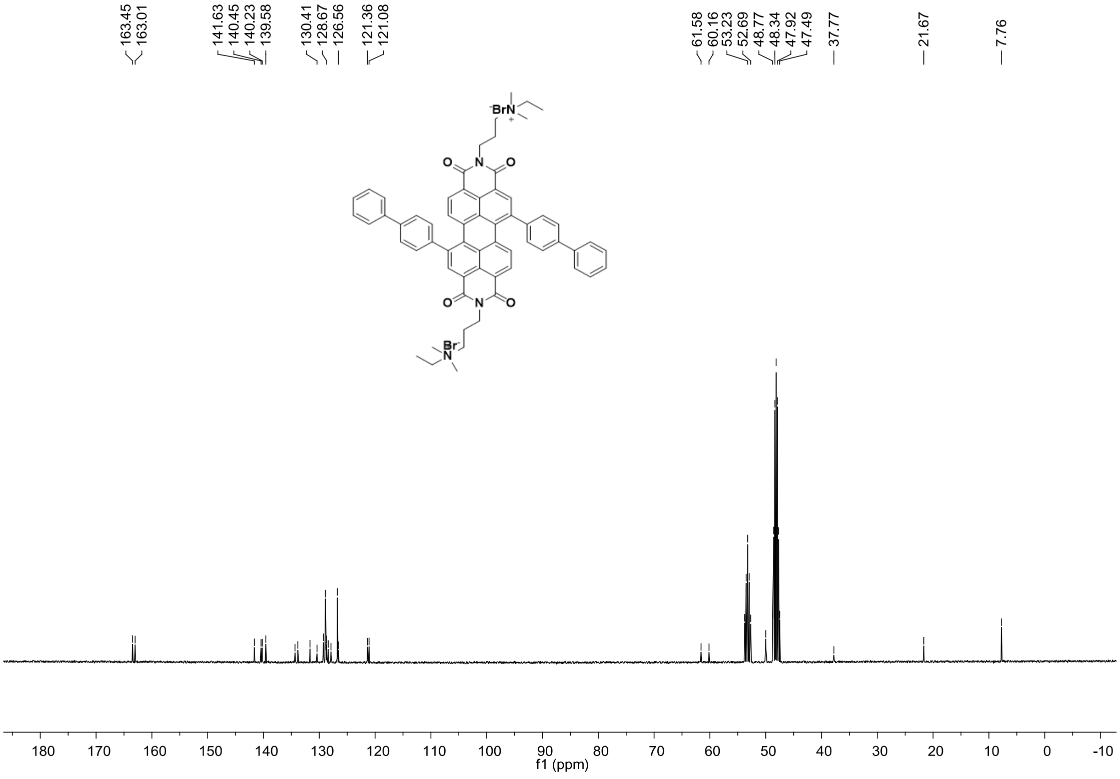

Figure S51. ^{13}C NMR spectrum of compound **14** in the mixture solvent of CD_2Cl_2 and CD_3OD.

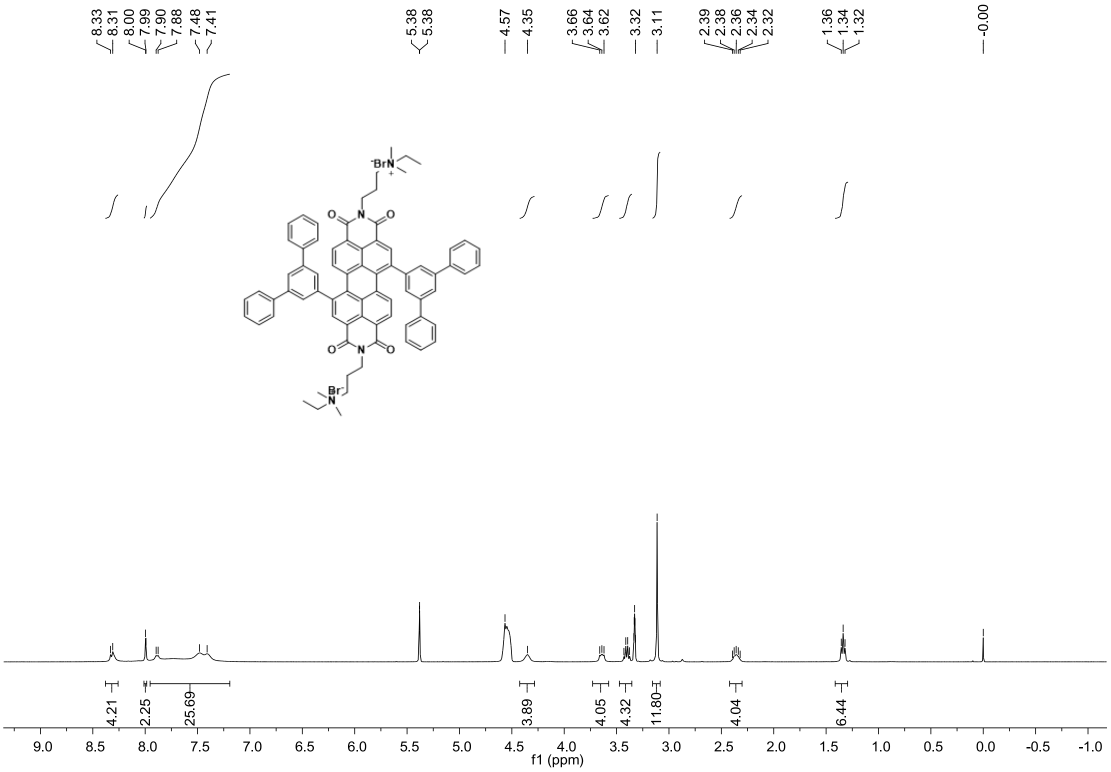

Figure S52. ^{1}H NMR spectrum of compound **15** in the mixture solvent of CD_2Cl_2 and CD_3OD.

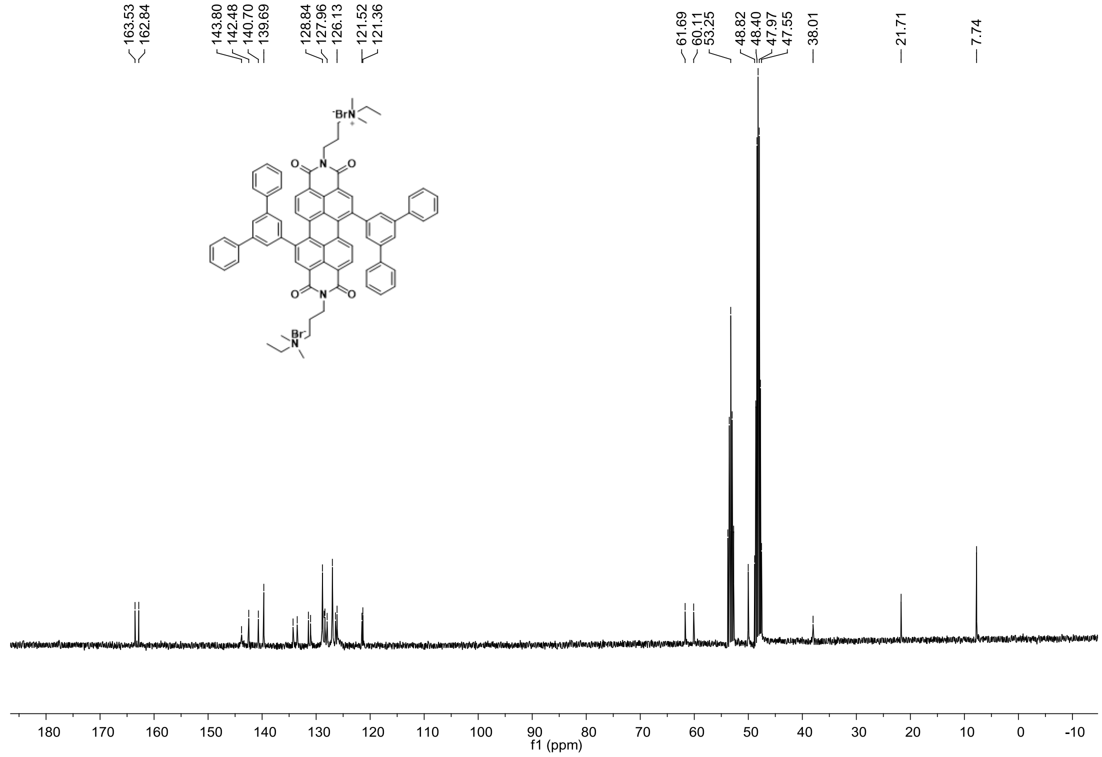

Figure S53. ^{13}C NMR spectrum of compound **15** in the mixture solvent of CD_2Cl_2 and CD_3OD.

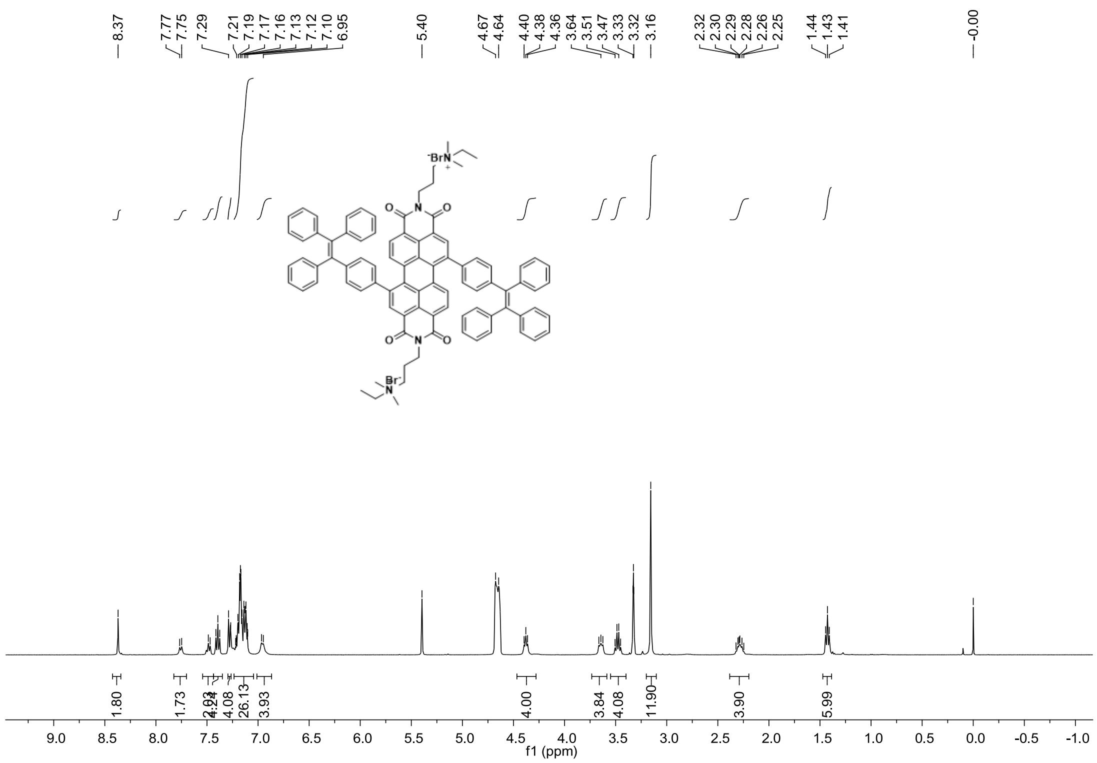

Figure S54. ^{1}H NMR spectrum of compound **16** in the mixture solvent of CD_2Cl_2 and CD_3OD.

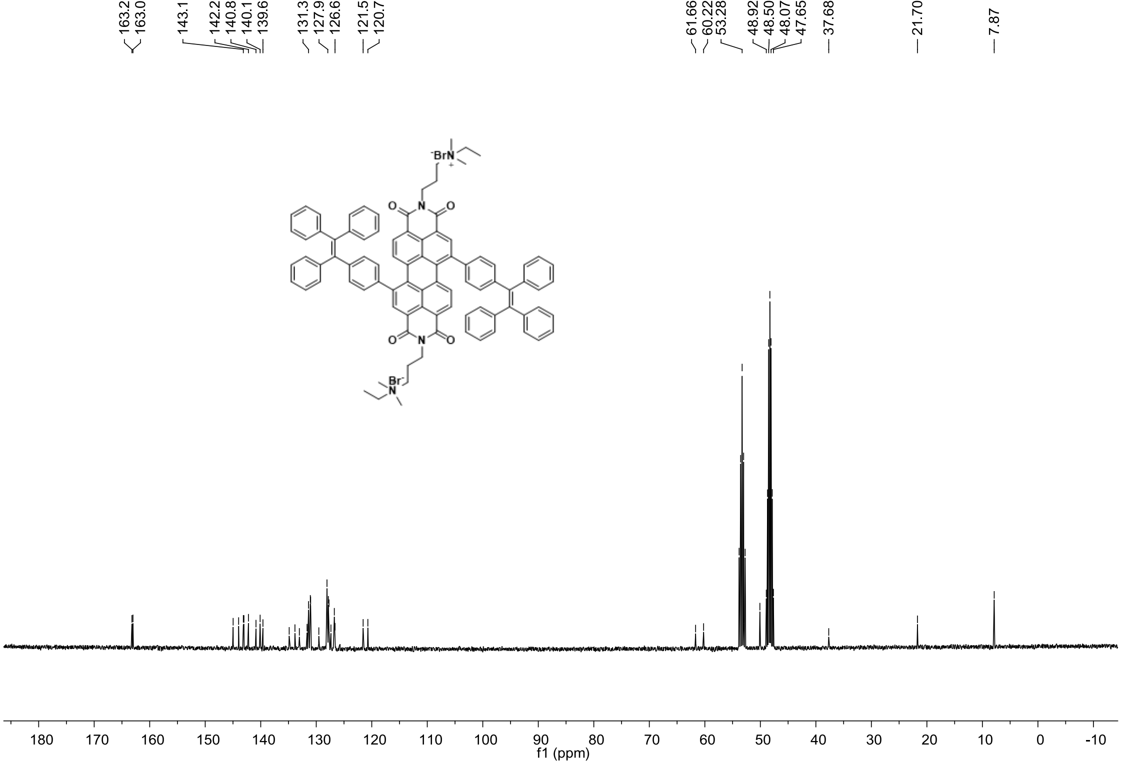

Figure S55. ^{13}C NMR spectrum of compound **16** in the mixture solvent of CD_2Cl_2 and CD_3OD.

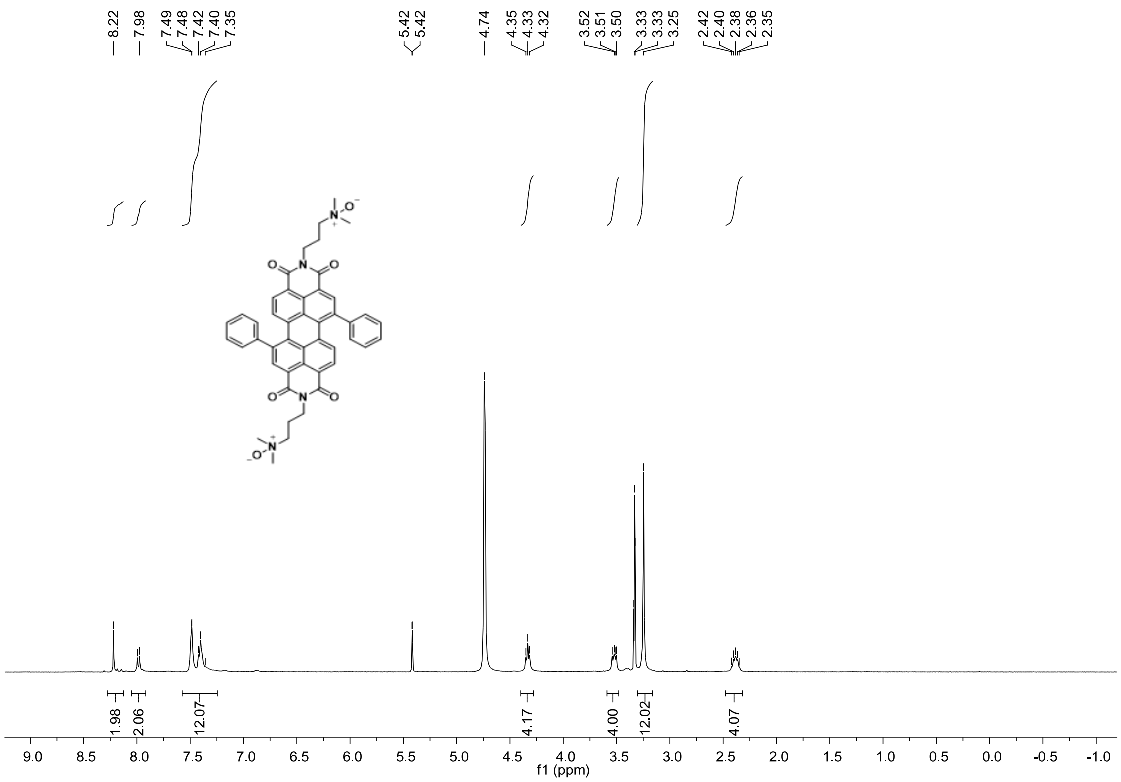

Figure S56. ^{1}H NMR spectrum of compound **17** in the mixture solvent of CD_2Cl_2 and CD_3OD.

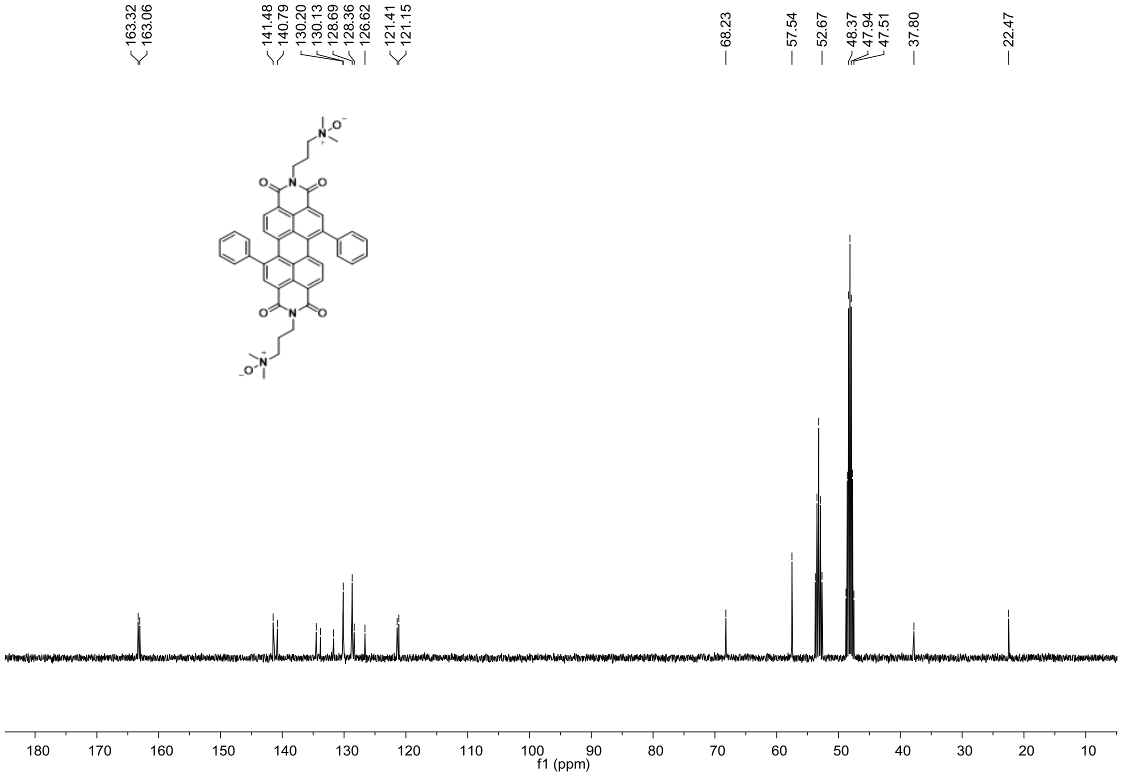

Figure S57. ^{13}C NMR spectrum of compound **17** in the mixture solvent of CD_2Cl_2 and CD_3OD.

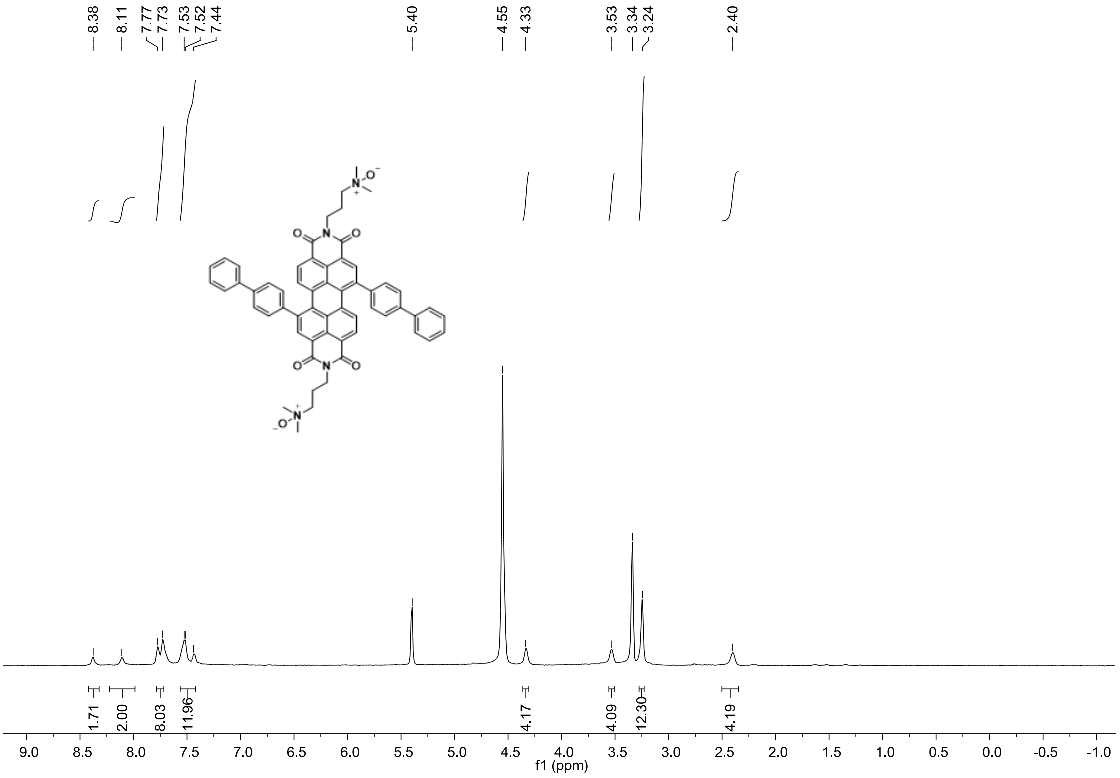

Figure S58. ^{1}H NMR spectrum of compound **18** in the mixture solvent of CD_2Cl_2 and CD_3OD.

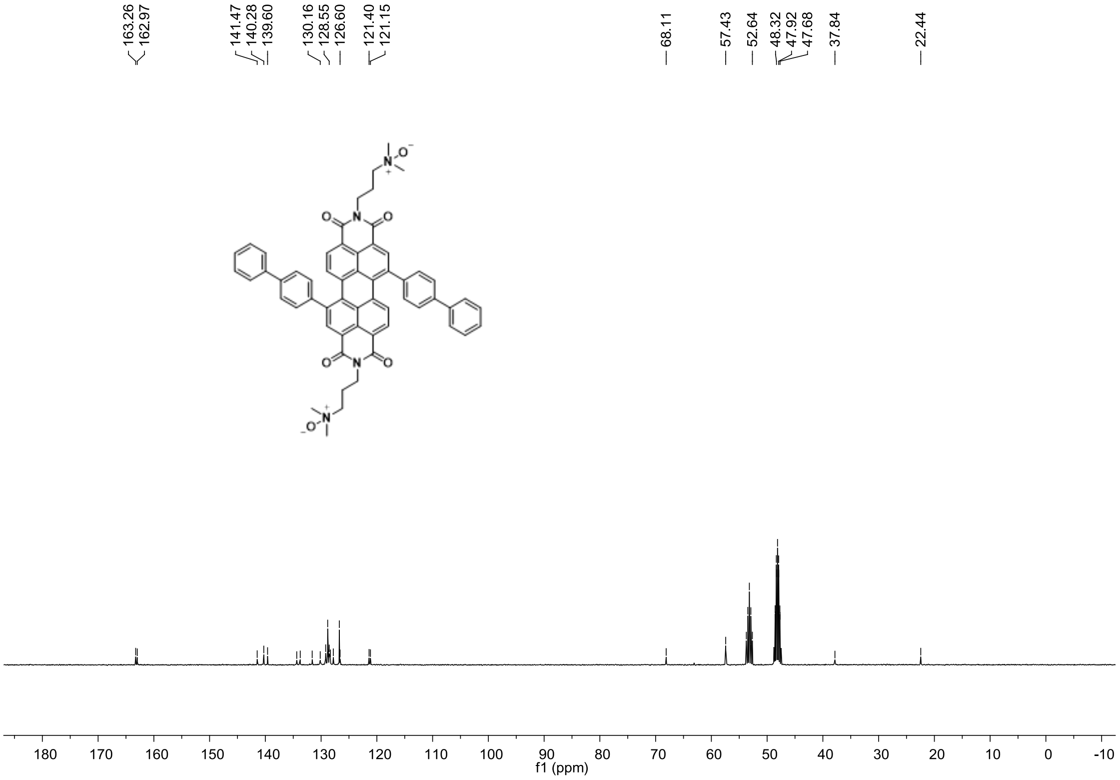

Figure S59. ^{13}C NMR spectrum of compound **18** in the mixture solvent of CD_2Cl_2 and CD_3OD.

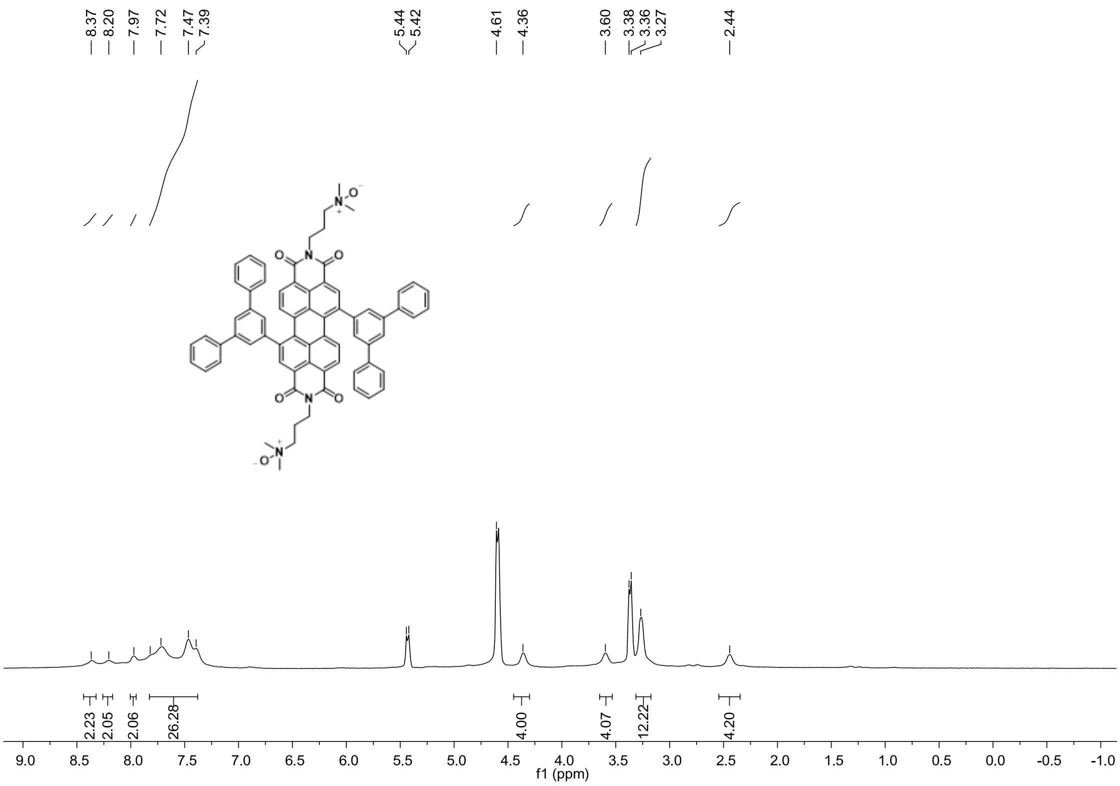

Figure S60. ^{1}H NMR spectrum of compound **19** in the mixture solvent of CD_2Cl_2 and CD_3OD.

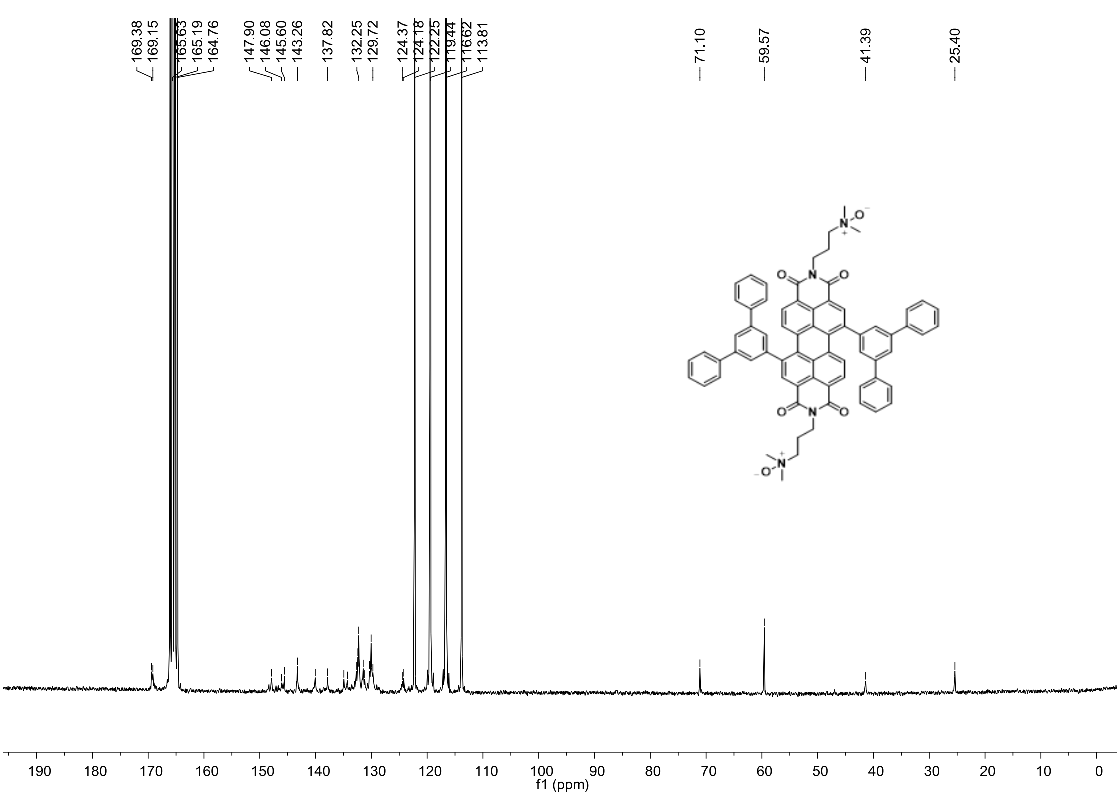

Figure S61. ^{13}C NMR spectrum of compound **19** in CF_3COOD.

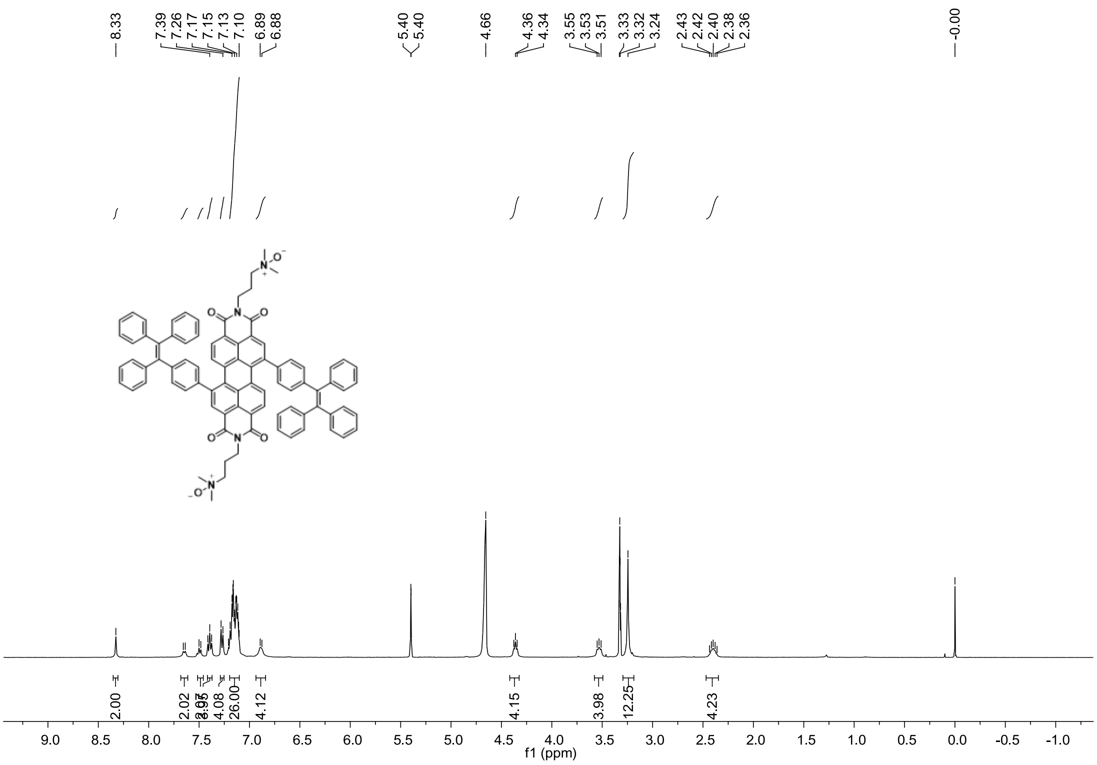

Figure S62. ^{1}H NMR spectrum of compound **20** in the mixture solvent of CD_2Cl_2 and CD_3OD.

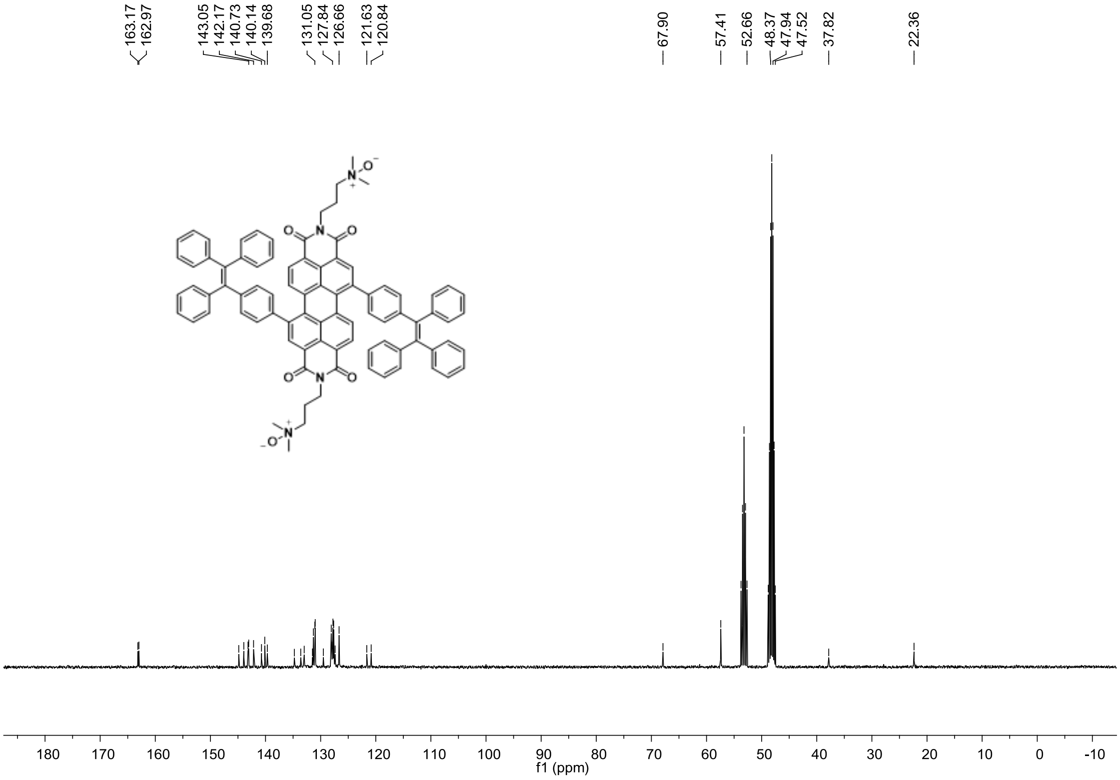

Figure S63. ^{13}C NMR spectrum of compound **20** in the mixture solvent of CD_2Cl_2 and CD_3OD.

5. High Resolution Mass Spectra

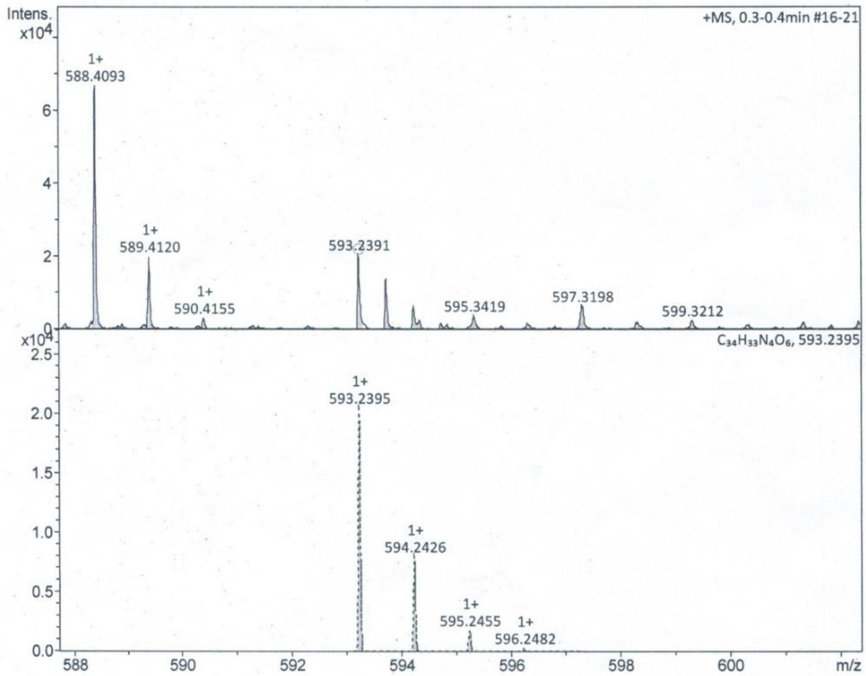

Meas. m/z	#	Ion Formula	Score	m/z	err [mDa]	err [ppm]	mSigma	rdb	e⁻ Conf	N-Rule	Adduct
593.239145	1	C34H33N4O6	100.00	593.239461	0.3	0.5	54.2	20.5	even	ok	M+H

Figure S64. High resolution mass spectrum of compound **8**.

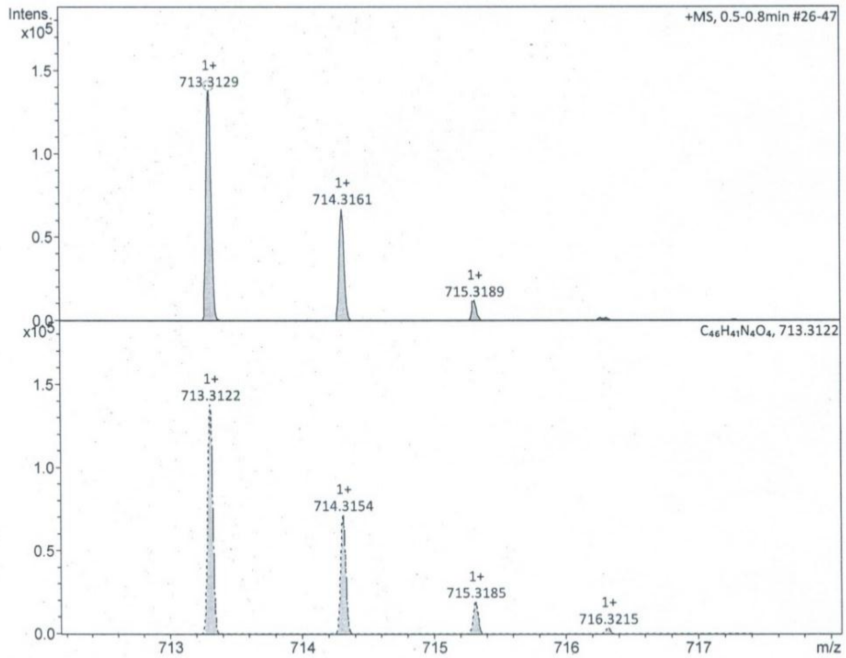

Meas. m/z	#	Ion Formula	Score	m/z	err [mDa]	err [ppm]	mSigma	rdb	e⁻ Conf	N-Rule	Adduct
713.312913	1	C46H41N4O4	100.00	713.312232	-0.7	-1.0	33.4	28.5	even	ok	M+H

Figure S65. High resolution mass spectrum of compound **9**.

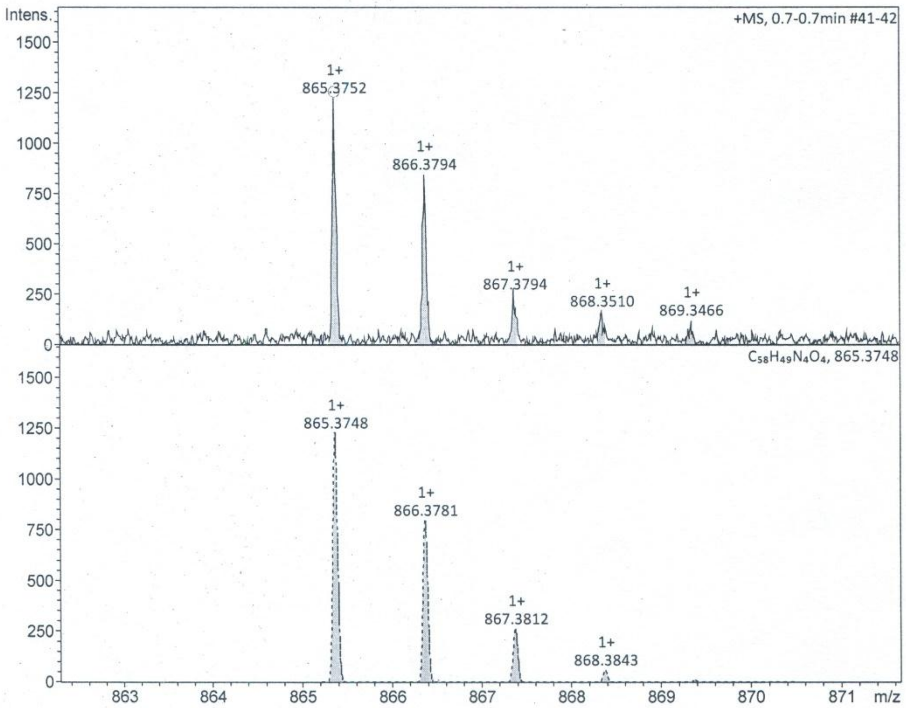

Meas. m/z	#	Ion Formula	Score	m/z	err [mDa]	err [ppm]	mSigma	rdb	e¯ Conf	N-Rule	Adduct
865.375236	1	C58H49N4O4	100.00	865.374832	-0.4	-0.5	32.2	36.5	even	ok	M+H

Figure S66. High resolution mass spectrum of compound **10**.

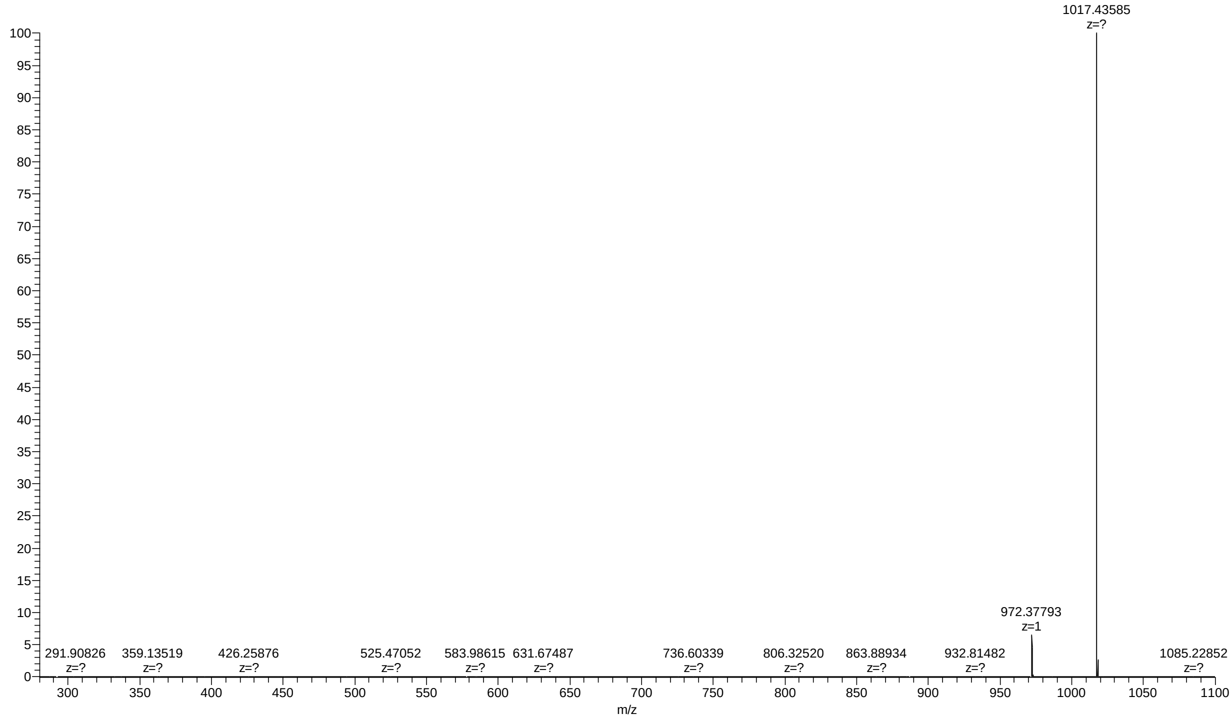

Figure S67. High resolution mass spectrum of compound **11**.

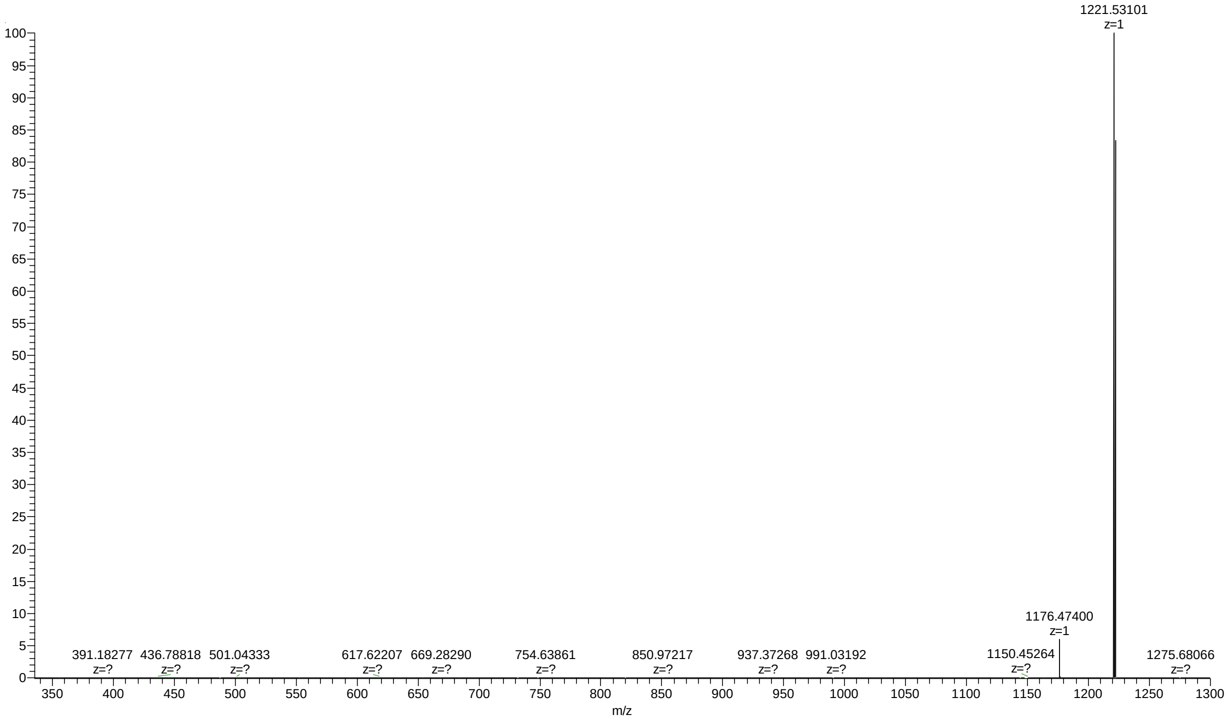

Figure S68. High resolution mass spectrum of compound **12**.

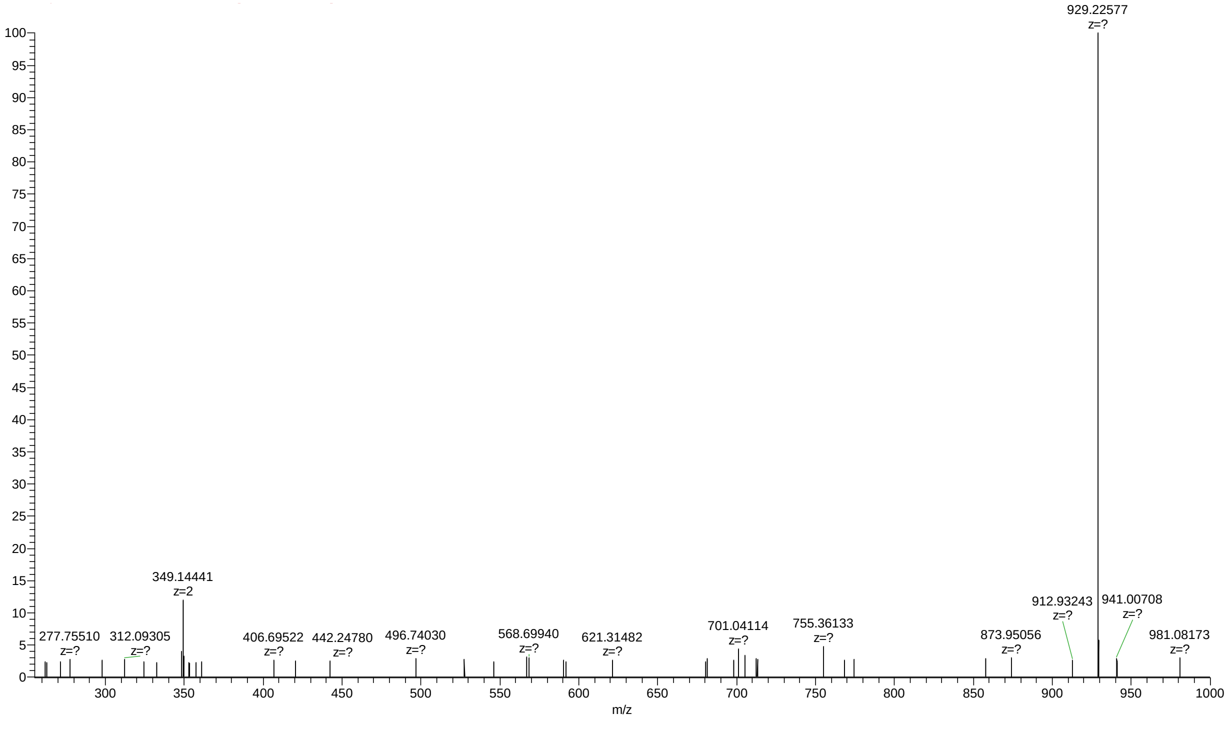

Figure S69. High resolution mass spectrum of compound **13**.

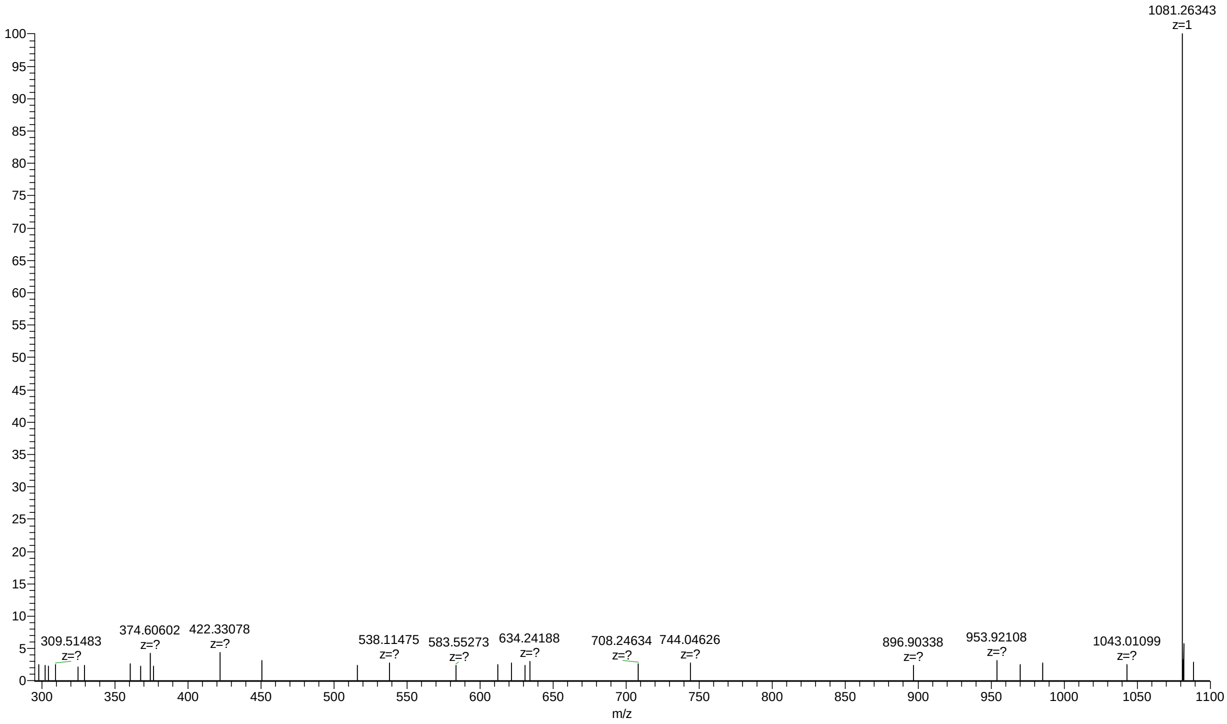

Figure S70. High resolution mass spectrum of compound **14**.

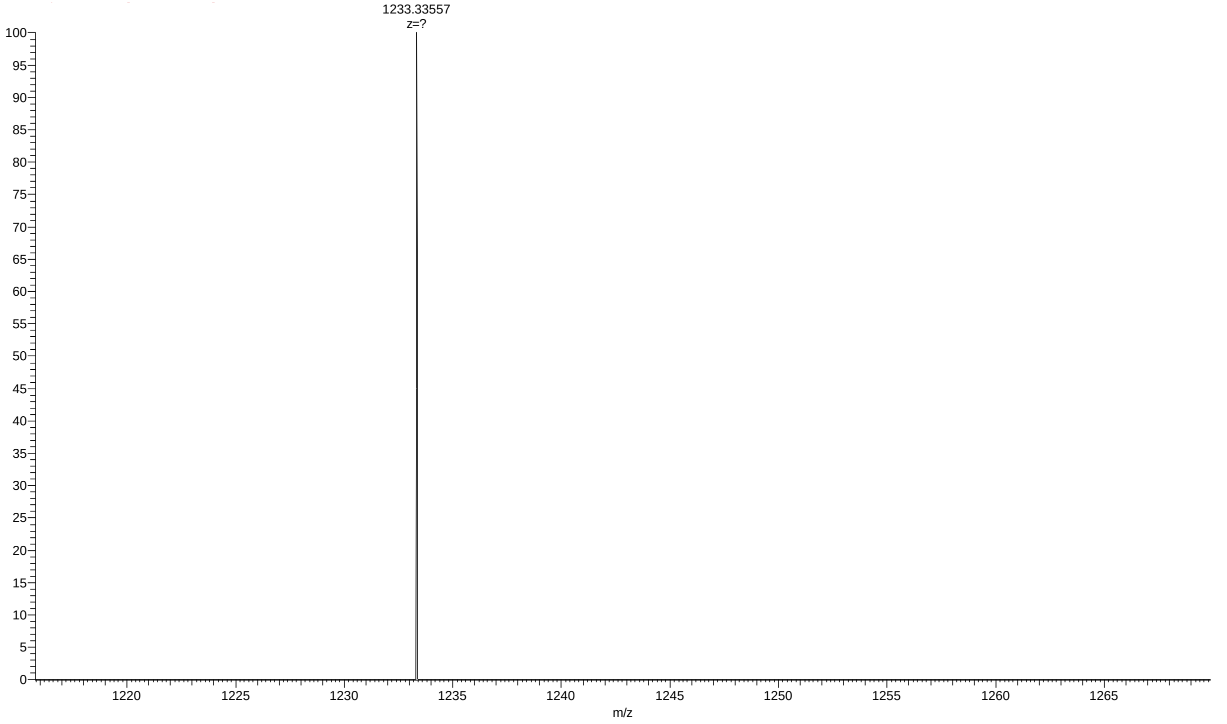

Figure S71. High resolution mass spectrum of compound **15**.

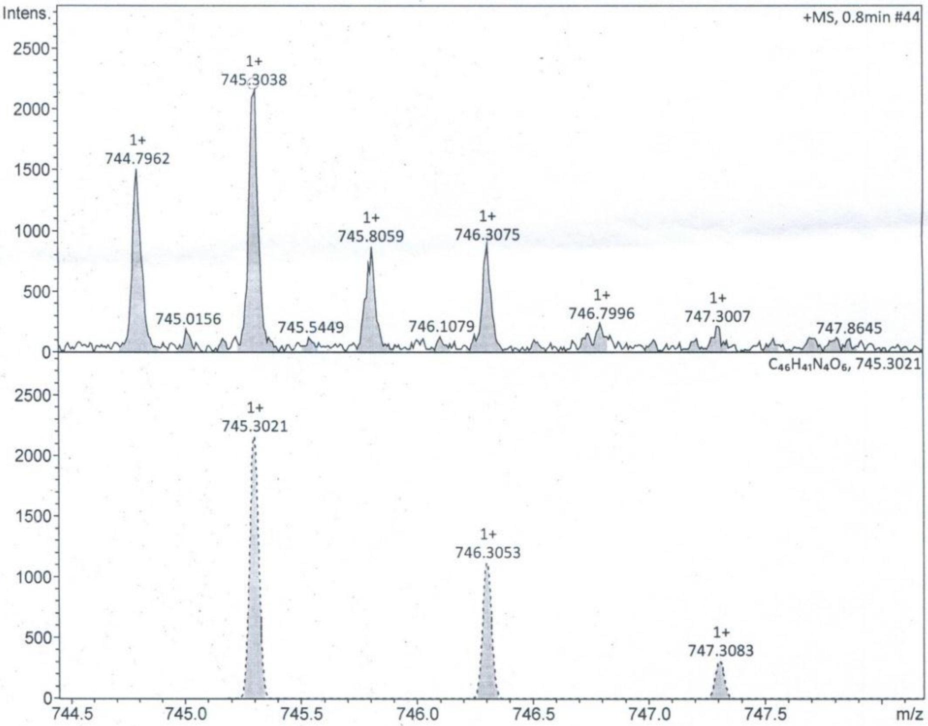

Meas. m/z	#	Ion Formula	Score	m/z	err [mDa]	err [ppm]	mSigma	rdb	e⁻ Conf	N-Rule	Adduct
745.303787	1	C46H41N4O6	100.00	745.302061	-1.7	-2.3	59.9	28.5	even	ok	M+H

Figure S72. High resolution mass spectrum of compound **17**.

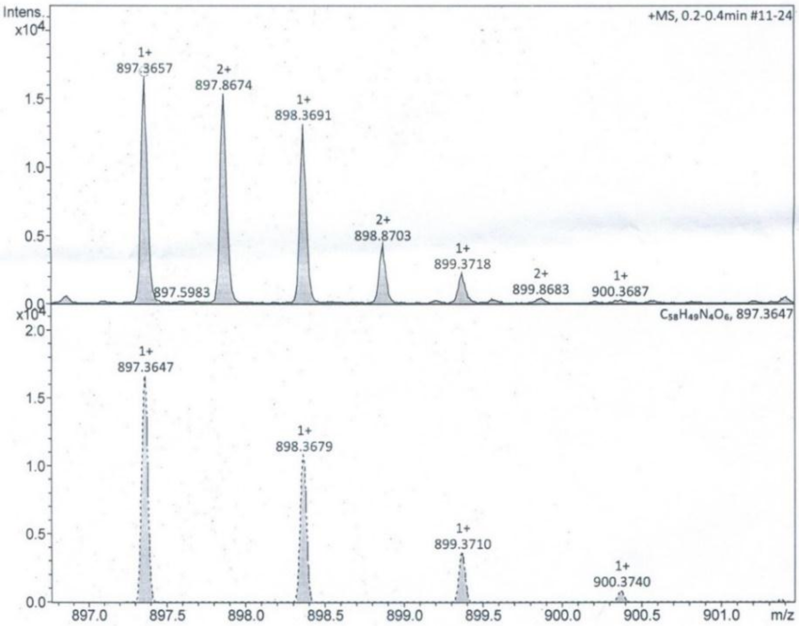

Meas. m/z	#	Ion Formula	Score	m/z	err [mDa]	err [ppm]	mSigma	rdb	e⁻ Conf	N-Rule	Adduct
897.365687	1	C58H49N4O6	100.00	897.364662	-1.0	-1.1	74.6	36.5	even	ok	M+H

Figure S73. High resolution mass spectrum of compound **18**.

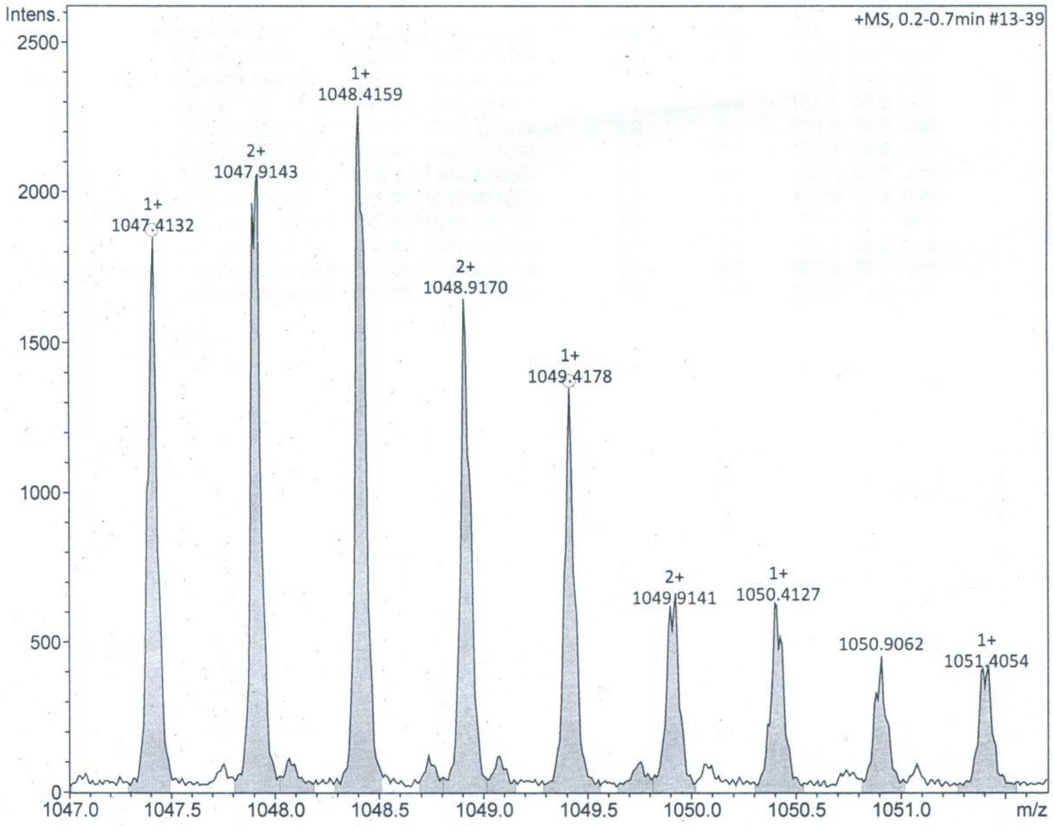

Figure S74. High resolution mass spectrum of compound **19**.

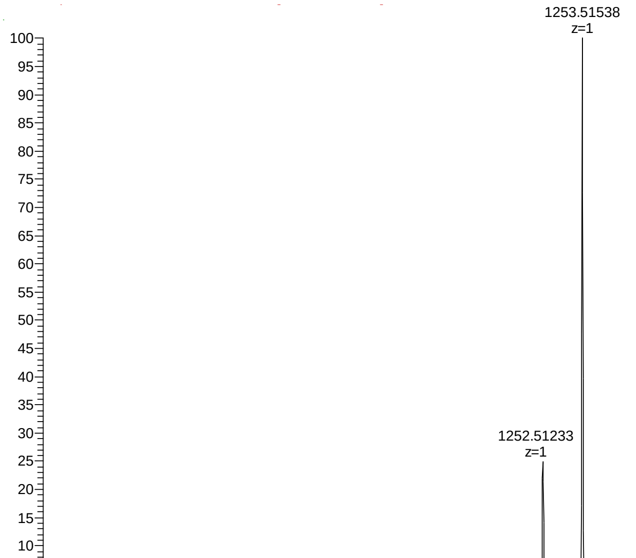

Figure S75. High resolution mass spectrum of compound **20**.

6. References

[1] Z.-G. Zhang, B. Qi, Z. Jin, D. Chi, Z. Qi, Y. Li and J. Wang, *Energy Environ. Sci.*, 2014, **7**, 1966-1973.

[2] X. Zhan, J. Zhang, S. Tang, Y. Lin, M. Zhao, J. Yang, H. L. Zhang, Q. Peng, G. Yu and Z. Li, *Chem. Commun.*, 2015, **51**, 7156-7159.

[3] A. Liang, H. Wang, Y. Chen, X. Zheng, T. Cao, X. Yang, P. Cai, Z. Wang, X. Zhang and F. Huang, *Dyes Pigm.*, 2018, **149**, 399-406.